AD-A096 473 RENSSELAER POLYTECHNIC INST TROY N Y DEPT OF MATERIA--ETC F/G 11/5
RELATION OF STRUCTURE TO PROPERTIES IN GRAPHITE FIBERS.(U)
JAN 81 R J DIEFENDORF, K J CHEN AFOSR-77-3436
UNCLASSIFIED RPI-5-24015 AFOSR-TR-81-0248 NL

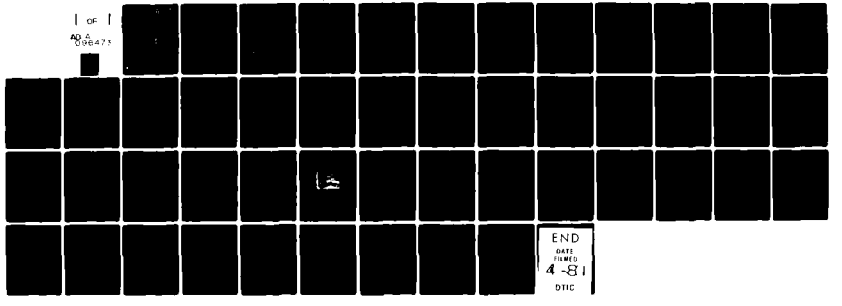

LEVEL II 8

FINAL TECHNICAL REPORT

"RELATION OF STRUCTURE TO PROPERTIES IN GRAPHITE FIBERS"

A.F.O.S.R.-77-3436 - R.P.I. #5-24015

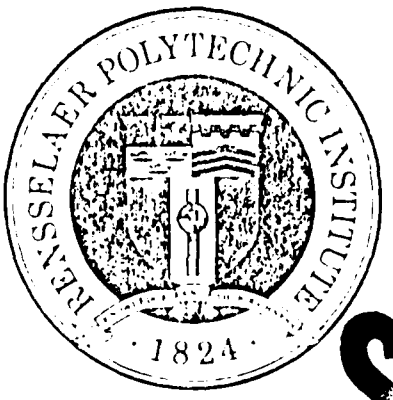

R. J. DIEFENDORF
(PRINCIPAL INVESTIGATOR)

K. J. CHEN
W. P. SEAGROVES
&
J. J-H. WANG

JANUARY 31, 1981

UNCLASSIFIED (9) Final Rept. 30 Sep 77 - 30 Sep 80

SECURITY CLASSIFICATION OF THIS PAGE (When Data Entered)

REPORT DOCUMENTATION PAGE

READ INSTRUCTIONS BEFORE COMPLETING FORM

(18) 1. REPORT NUMBER (19) AFOSR-TR-81-0248 | 2. GOVT ACCESSION NO. AD-A096 473 | 3. RECIPIENT'S CATALOG NUMBER

(6) 4. TITLE (and Subtitle)
Relation of Structure to Properties in Graphite Fibers.

5. TYPE OF REPORT & PERIOD COVERED
Final
9/30/77 - 9/30/80

6. PERFORMING ORG. REPORT NUMBER

(10) 7. AUTHOR(s)
R. J. Diefendorf, Principal Investigator
K. J. Chen
W. P. Scaproves
J. J-H. Wang

(15) 8. CONTRACT OR GRANT NUMBER(s)
AFOSR-77-3136

9. PERFORMING ORGANIZATION NAME AND ADDRESS
Materials Engineering Department
Rensselaer Polytechnic Institute
Troy, New York 12181

10. PROGRAM ELEMENT, PROJECT, TASK AREA & WORK UNIT NUMBERS
(16) 2305/A5
61102F
(17) A5

11. CONTROLLING OFFICE NAME AND ADDRESS
Air Force Office of Scientific Research/NC (11)
Bldg. 410, Bolling AFB, D.C. 20332

12. REPORT DATE
21 January 1981

13. NUMBER OF PAGES
17

14. MONITORING AGENCY NAME & ADDRESS(if different from Controlling Office)
(12) 14 ?

15. SECURITY CLASS. (of this report)
UNCLASSIFIED

15a. DECLASSIFICATION/DOWNGRADING SCHEDULE

16. DISTRIBUTION STATEMENT (of this Report)
(14) RPI-5-24015

Approved for public release; distribution unlimited.

17. DISTRIBUTION STATEMENT (of the abstract entered in Block 20, if different from Report)

18. SUPPLEMENTARY NOTES

19. KEY WORDS (Continue on reverse side if necessary and identify by block number)
Carbon Fibers, Composites

20. ABSTRACT (Continue on reverse side if necessary and identify by block number)
See reverse side of this sheet....

DD FORM 1 JAN 73 1473 EDITION OF 1 NOV 65 IS OBSOLETE

UNCLASSIFIED

SECURITY CLASSIFICATION OF THIS PAGE (When Data Entered)

302125

The axial properties of carbon fibers were found to correlate well with preferred orientations determined by either x-ray diffraction or optical techniques. High modulus carbon fibers were found to have significant gradients in preferred orientation. For HMS fiber, the modulus of the surface layers is about twice the average fibers modulus, while the interior modulus is only about one-half the average. This modulus gradient suggests that higher modulus fibers, with good strength, could be produced, if the modulus at the interior of these fibers could be increased.

The gradient in preferred orientation produces high residual stresses in HMS fibers. While the high surface compressive stresses minimize the effect of surface flaws, the high axial tensile stresses in the interior may decrease strength by causing fracture to initiate at flaws in the interior rather than at the surface. Similarly, the high axial compressive stressed outer layers of a fiber may initiate buckling when the fiber is compressively loaded. Modifications of the residual stress pattern might allow increased tensile and/or compressive strengths to be obtained in high modulus carbon fibers. Many correlations between properties and fiber diameter, reported in the past, may be in error because it is very difficult to determine the fiber diameter precisely and accurately.

REVIEW OF ACCOMPLISHMENTS

* The axial properties of carbon fibers were found to correlate well with preferred orientations determined by either x-ray diffraction or optical techniques.

* High modulus carbon fibers were found to have significant gradients in preferred orientation. For HMS fiber, the modulus of the surface layers is about twice the average fibers modulus, while the interior modulus is only about one-half the average. This modulus gradient suggests that higher modulus fibers, with good strength, could be produced, if the modulus at the interior of these fibers could be increased.

* The gradient in preferred orientation produces high residual stresses in HMS fibers. While the high surface compressive stresses minimize the effect of surface flaws, the high axial tensile stresses in the interior may decrease strength by causing fracture to initiate at flaws in the interior rather than at the surface. Similarly, the high axial compressive stressed outer layers of a fiber may initiate buckling when the fiber is compressively loaded. Modifications of the residual stress pattern might allow increased tensile and/or compressive strengths to be obtained in high modulus carbon fibers.

* Many correlations between properties and fiber diameter, reported in the past, may be in error because it is very difficult to determine the fiber diameter precisely and accurately.

PUBLICATIONS

1) Residual Stresses in High Modulus Carbon Fibers, W. C. Stevens, J. H. Wang and R. J. Diefendorf, Carbon '80, pp. 598-602, Deutchen Keramischen Gesellshaft, Bad Honnef, West Germany, 1980.

(TO BE PUBLISHED:)

2) Optical Properties of Carbon Fibers, W. P. Seagroves and R. J. Diefendorf.

3) Oxidation Kinetics of Carbon Fibers, K. J. Chen and R. J. Diefendorf.

4) Modulus/Diameter and Strength/Diameter Correlations in Carbon Fibers, K. J. Chen and R. J. Diefendorf.

5) The Effect of Residual Stress on the Transverse Optical Microstructure of Carbon Fibers, K. J. Chen and R. J. Diefendorf.

TABLE OF CONTENTS

I. INTRODUCTION

The axial properties of carbon fibers such as modulus, coefficient of thermal expansion, and strength, are easily measured in the as-received state. However, large changes in the fiber properties can occur during processing of carbon/carbon composites, and the fiber properties in the finished carbon/carbon composite are not easily determined.

Two methods of measuring preferred orientation on carbon fibers in finished carbon/carbon composites could be used with crystal properties to correlate with the axial properties:

(1) X-ray diffraction

(2) Optical.

While x-ray diffraction has been used for more than a decade to measure preferred orientation in carbon fibers, it is often limited by the requirement to use a bundle of fibers to obtain the necessary intensity and, in any case, it averages the preferred orientation throughout the fibers.

A major advantage of x-ray diffraction is that the intensity from a diffracting plane drops drastically for slight misorientations. Hence, the corrected intensity plot accurately describes the exact orientation position of the basal planes within the fiber. This makes the method very sensitive to small changes in the actual distribution (shape of the curve).

Quantitative optical microscopy has been used as a second technique for determining preferred orientation. The optical activity is observed using light reflected off a polished fiber sample. Information is required on both axial and transverse microstructure, and this is most easily obtained from a low angle oblique section. Preferred orientations on areas

as small as $1\mu^2$ can be measured, and the variation can be measured across the fiber diameter. Hence, changes in modulus across a fiber can be determined. However, optical activity is not sensitive to small tilts in basal planes in the plane of the polished surface. Therefore, two samples could have identical optical activity, but different x-ray preferred orientations and physical properties such as modulus.

Optical studies indicate a gradient in preferred orientation across the fiber diameter, and residual stresses should be present which may alter the strength of a brittle material such as a carbon fiber. The small effect of surface abrasion on the strength of high modulus carbon fibers also suggests compressive axial residual stresses at the fiber surface. Hence, studies were also performed to determine residual stress in carbon fibers.

II. EXPERIMENTAL

(A) X-ray diffraction

(1) Technique

A bundle of fibers was attached to an annular type sample holder so that they covered the center hole of the annulus. The fibers were kept nearly parallel by dipping them in acetone and allowing the capillary action to draw the fibers together. The acetone also reacted with a thin film of acetone plastic on the surface of the sample holder and fiber arrangement is shown in Figure 1. The sample holder was rotated (in the "ϕ" direction) by a clock motor to determine preferred orientation. The holder was placed in the diffractometer so that the axis of rotation in the plane was determined by the incident and diffracted beam, diffractometer plane, as in Figure 2. The axis of rotation was also kept at an angle of θ degree to the incoming beam. The specimen was then

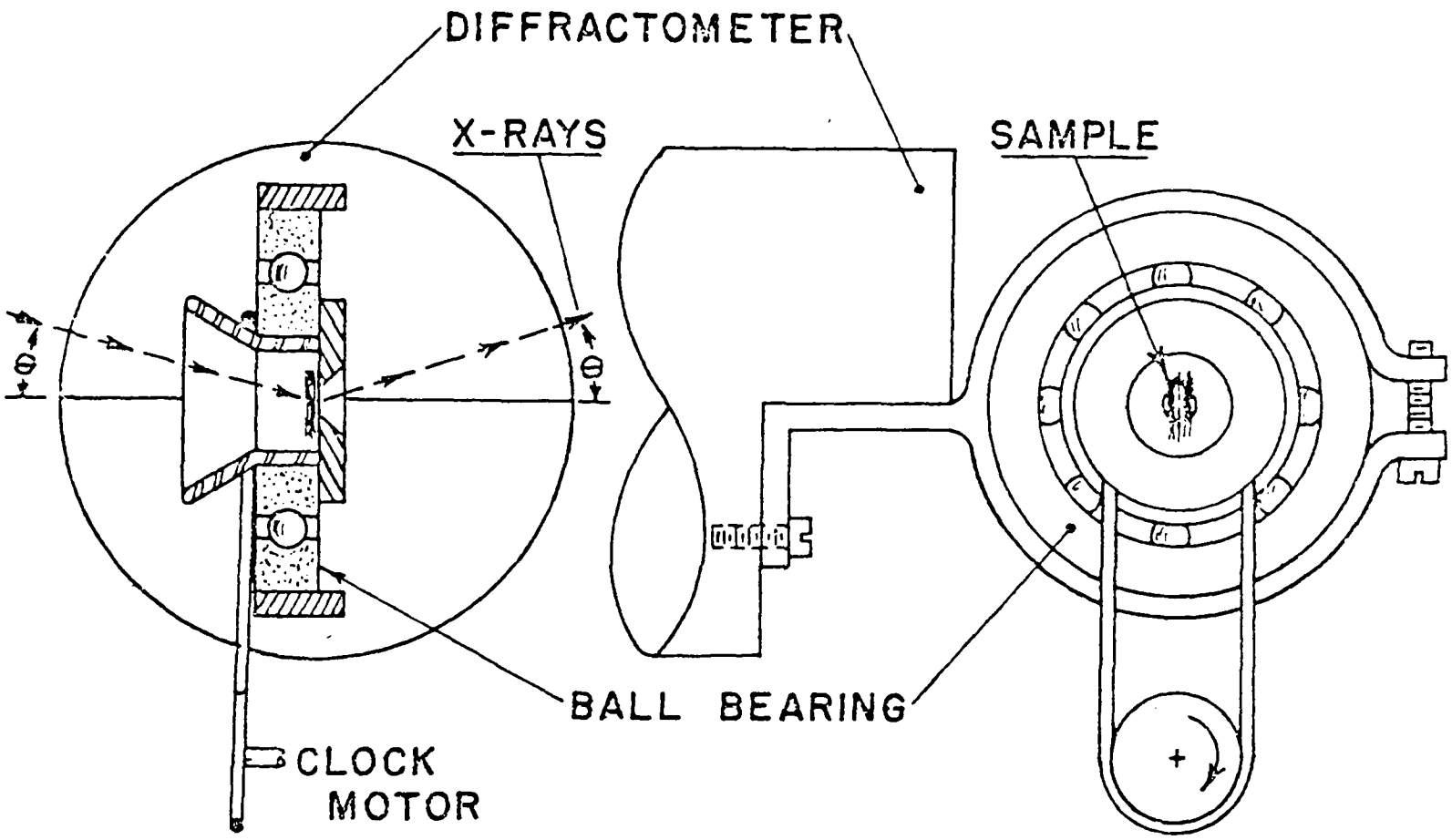

Figure 1. The Sample holder used to rotate the carbon fibers in the x-ray beam.

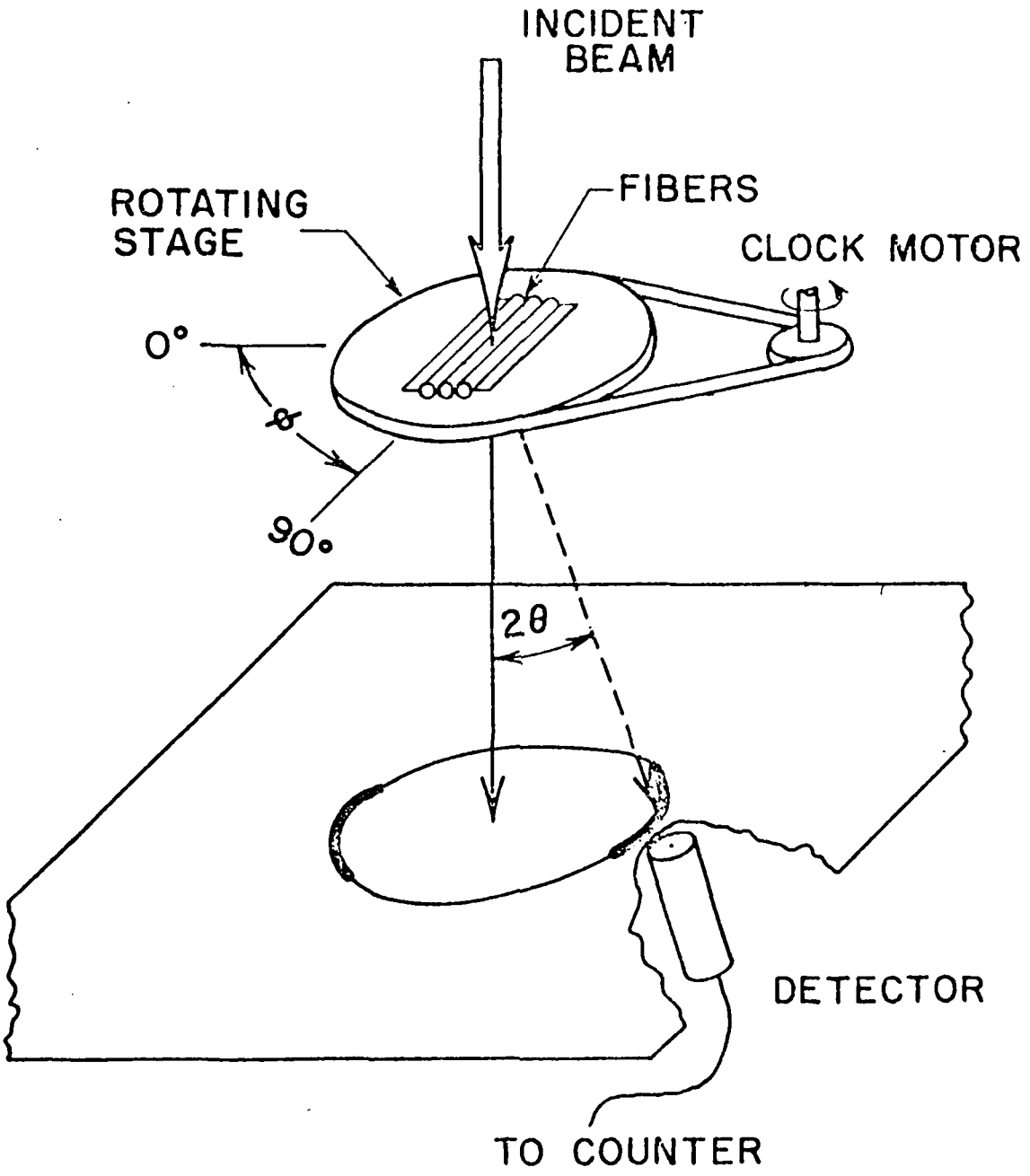

Figure 2. The Schematic view of the x-ray diffractometer apparatus with the rotating specimen stage.

positioned for a ϕ intensity maximum by making the bundle axis perpendicular to the diffractometer plane. The 2θ scans were then made to determine the values at which 2θ should be set for the ϕ scans. With 2θ property set, the intensity of the 0002 peak in the ϕ scans was a maximum. The actual figures in reciprocal space were measured with a Norelco diffractometer and x-ray unit fitted with a copper K_α radiation source. The diffractometer provided the usual 2θ scan with a proportional counter as a detector. The specially designed and constructed rotation stage was used to enable the ϕ direction to be scanned. The output data took the form of strip charts which were plots of intensity versus ϕ or 2θ, as shown in Figure 3.

(2) Corrections

We must make corrections for crystallite size and other factors which affected the shape of the 0002 diffraction arcs. The width of the peak in the ϕ direction is contributed by the following:

i) Preferred orientation of the basal planes with respect to the fiber axis of the graphite crystallite within the fibers.

ii) Orientation of the sample fibers in the plane of the sample holder.

iii) Crystallite size of the graphite crystallites in the 1000 direction or La.

iv) Pure instrument broadening from the geometry of the diffractometer.

(B) Optical microscopy

(1) Metallographic preparation

Fibers were mounted in epoxy in two ways: perpendicular and parallel to the final polished surface. Then, the samples were polished to get end cross sections and longitudinal sections.

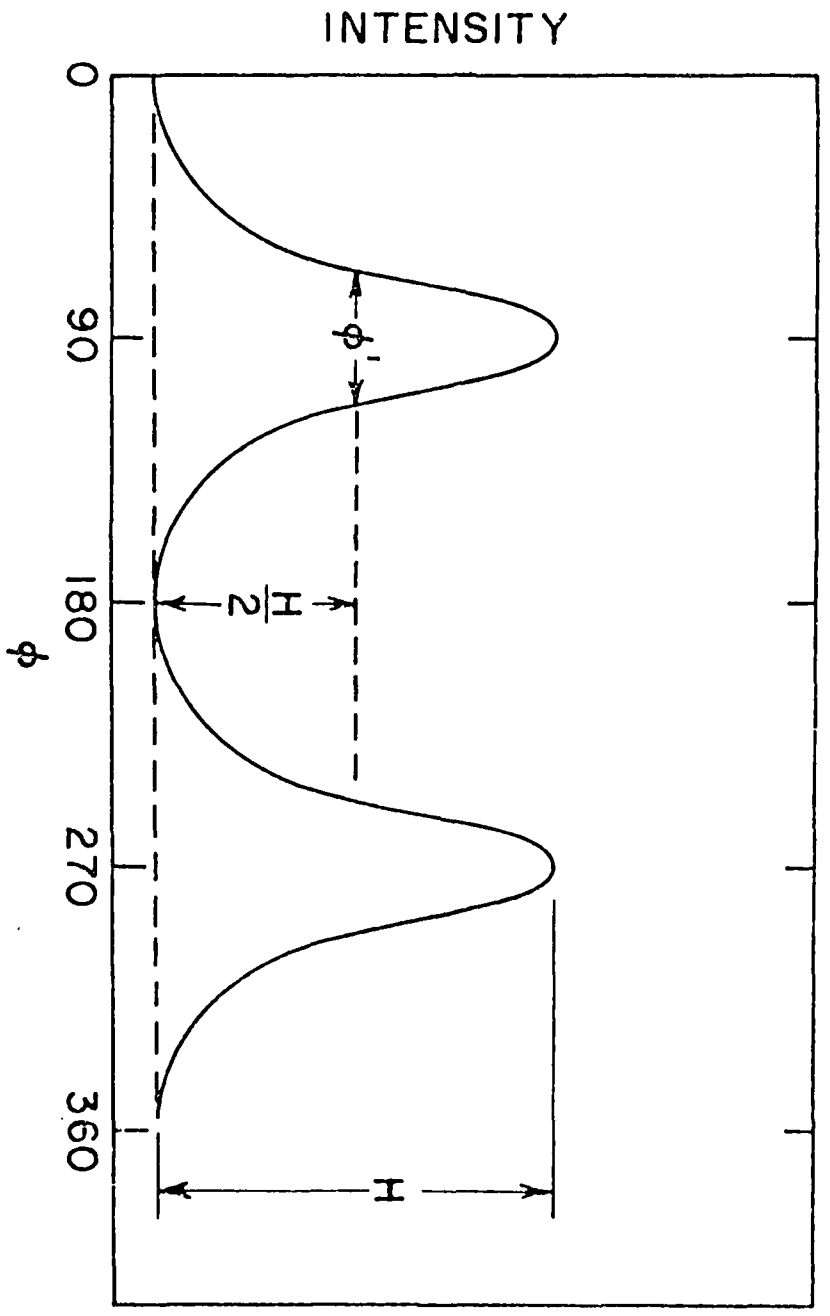

Figure 3. Two symmetrical peaks measured from preferred orientation measurement.

(2) Measurement

These measurements were determined with a Leitz MPV system which can measure light from a small region. Preferred orientations on fiber areas as small as $1\mu^2$ can be measured, and this allows the variation in preferred orientation across a fiber to be determined.

(C) Residual stress measurements

(1) Removal of surface layers

The surface layers of carbon fibers were successfully removed by gaseous oxidation or ion milling. For air oxidation, the fibers were cleaned with THF (tetra-hydrofuran) in an ultrasonic cleaner. The cleaned fibers were then dried, and placed into furnace for oxidation at 580°C, 630°C, 680°C, 730°C and 760°C for different periods of time from 10 minutes to 3 hours. Fibers to be ion thinned were mounted onto a metal washer which was fastened to the stage of ion milling apparatus. The stage rotated between two opposed sputtering guns operating at 6000V and 50 μa which permitted more uniform sputtering of the fibers. The fibers were thinned to different reduced diameters by varying the lengths of furnace or sputtering time.

(2) Measurement of modulus gradient

Fibers (2.5 cm gauge length) were mounted individually for mechanical testing and a segment of the fiber was saved for diameter measurement. A compliance correction for the tensile tester was used in the modulus determinations, but is 10% or less in magnitude.

(3) Measurement of residual strain

A technique was developed to measure contraction of fiber segments less than 0.5 cm in length. A reference fiber was mounted straight and a specimen fiber was mounted in a circular arc on a washer

as shown in Figure 4a. Both fibers were then sputtered and the contraction of the specimen fiber was measured, Figure 4b. As compressive surface layers were removed during sputtering, the fiber shrank. The straight reference fiber naturally remained stationary. However, the arced fiber drew away from the reference fiber as the arced fiber contracted. The measurement of separation distance between the reference fiber and the arced fiber was an indirect measurement of the strain within the specimen fiber.

III. RESULTS AND DISCUSSION

(A) X-ray diffraction and preferred orientation

(1) Theory

In 1956, Bacon[1] developed a technique to measure the "anisotropy factor" and to estimate the degree of preferred orientation in graphite. He then related preferred orientation to the mechanical properties of graphite prepared by extrusion and pressing. Ruland[2] rotated fiber samples in the ϕ direction and measured the x-ray diffraction intensity variation of the (0002) peak along this ϕ direction to get a texture parameter function, $g(\phi)$. This function can be used into the equation he developed to estimate the modulus in the direction of the fiber axis. Butler[3] used the same method to measure the preferred orientation for several commercial carbon fibers and suggested the parameter, $\phi_{1/2}$, which is the width at half-maximum peak height of the I_{0002} versus ϕ distribution curve, can be used to estimate the preferred orientation within the fiber.

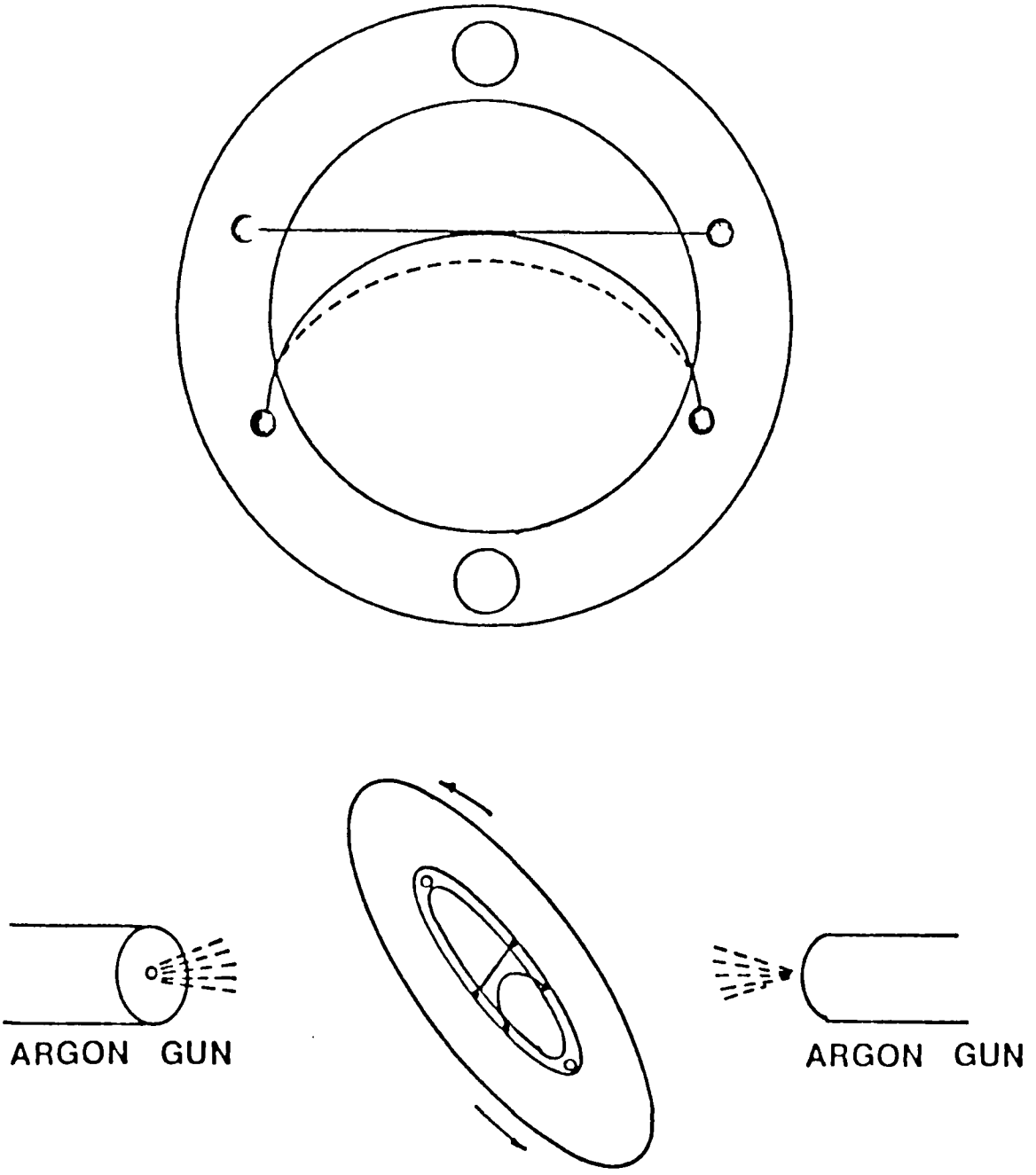

FIGURE 4 - Measurement technique of fiber contraction as a result of ion milling surface layers away.

(2) Results

The modulii of carbon fibers versus half-width follow along two curves, Figure 5. In one set, for fibers heated to high temperatures, there is a lower modulus for a given preferred orientation. In the second set, fibers are heated to lower heat-treatment temperatures and the larger the difference from the first curve, the lower the heat-treatment temperature. This deviation is probably caused by the increase in basal plane shear modulus at lower heat-treatment temperature. In either case, there is a correlation, and for high heat-treatment temperatures, such as used in carbon/carbons, the relationship can be assumed to follow the lower curve.

A similar plot, Figure 6, using the texture parameter illustrates again that high heat-treatment temperature results in a lower modulus for a given preferred orientation. The agreement for high-temperature heat-treated fibers and calculated values based on constant stress, graphite single crystal elastic constants, and the texture parameter is excellent. Deviation for lower temperatures heat-treatment fibers can be explained again by an increase in shear modulus.

The observed x-ray intensity is often well fitted by the texture parameter as shown by the HTS fibers and most others, Figure 7. However, for some fibers, notably the Fortifil T series, significant deviation occurs and would require numerical evaluation for proper estimation of modulus.

FIGURE 5:

MODULUS VS. WIDTH AT HALF MAXIMUM (002)
CARBON FIBERS

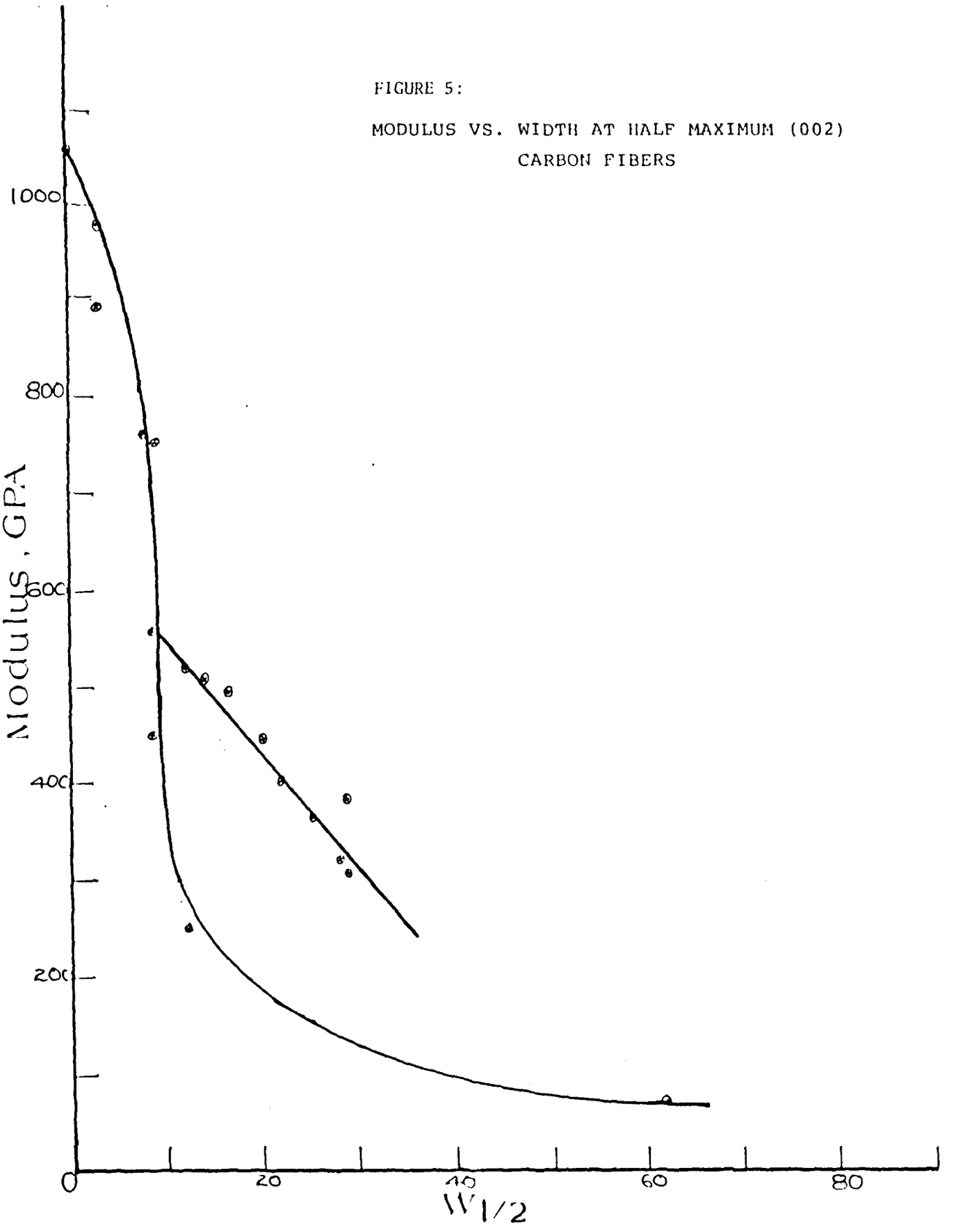

FIGURE 6

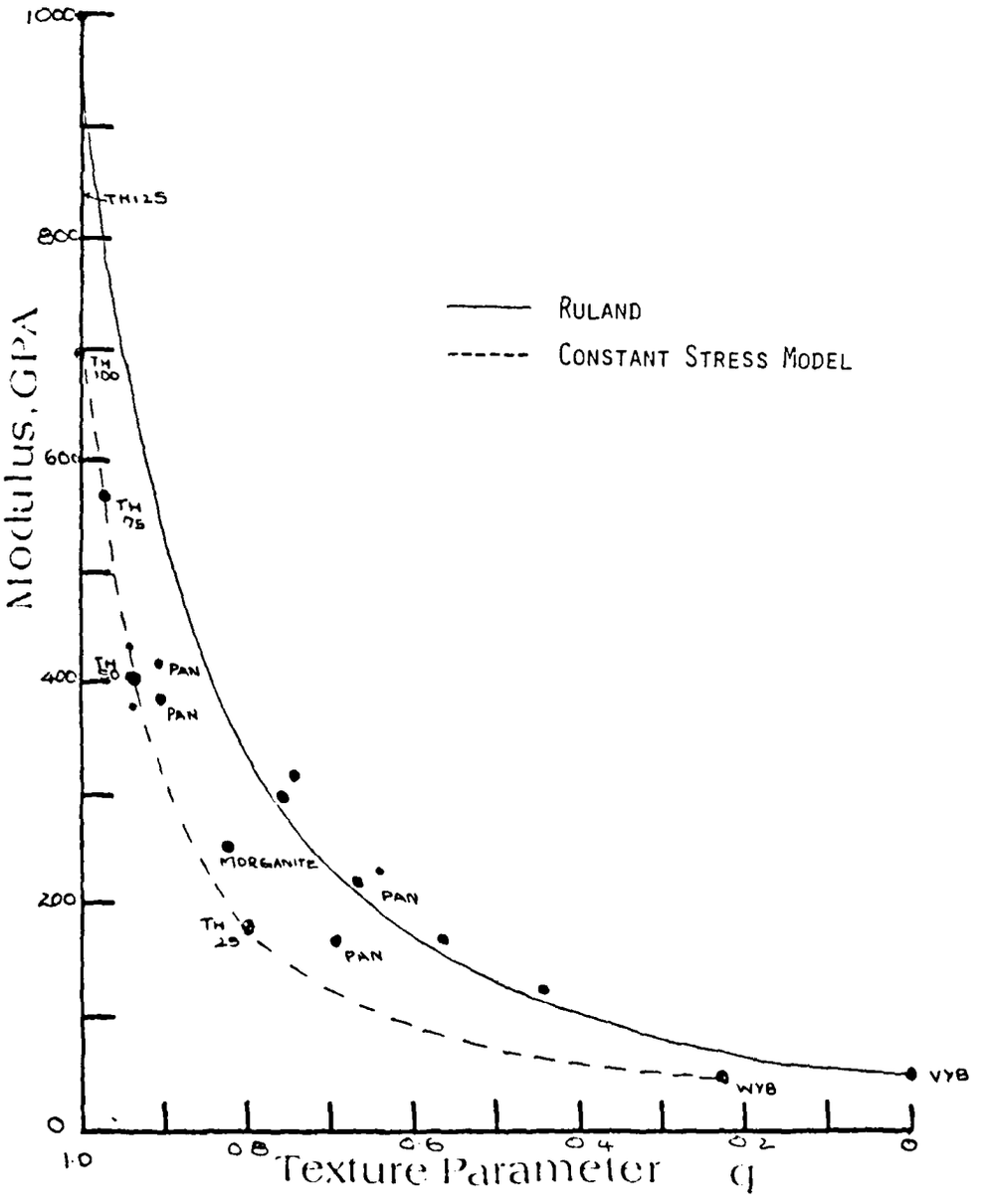
1000
800
600
400
200
0
Modulus, GPA
TH125
TH 100
TH 75
TH 50
PAN
PAN
MORGANITE
PAN
TH 25
PAN
WYB
VYB
1.0
0.8
0.6
0.4
0.2
0
Texture Parameter q
RULAND
CONSTANT STRESS MODEL

FIGURE 7

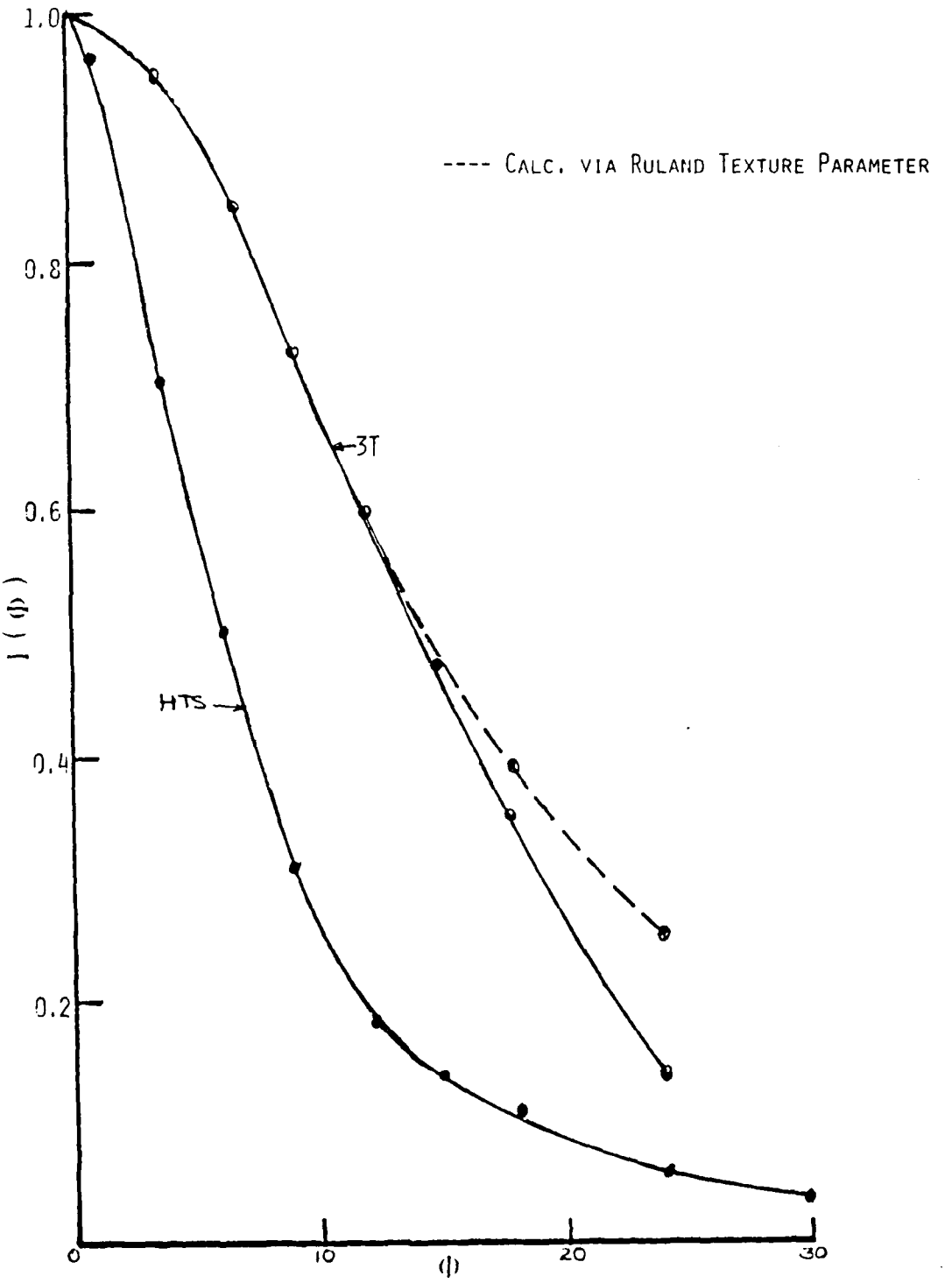
1.0
0.8
0.6
0.4
0.2
I (Φ)
0
10
20
30
Φ
3T
HTS
---- CALC. VIA RULAND TEXTURE PARAMETER

(3) Comment on previous work

(i) No matter what kind of fibers they are, the higher the preferred orientation, the higher the modulus.

(ii) At $\phi = 0°$ only small fractions of the fibers have been diffracted so the intensity received is a little too low. That means actual preferred orientation for the fibers is much higher.

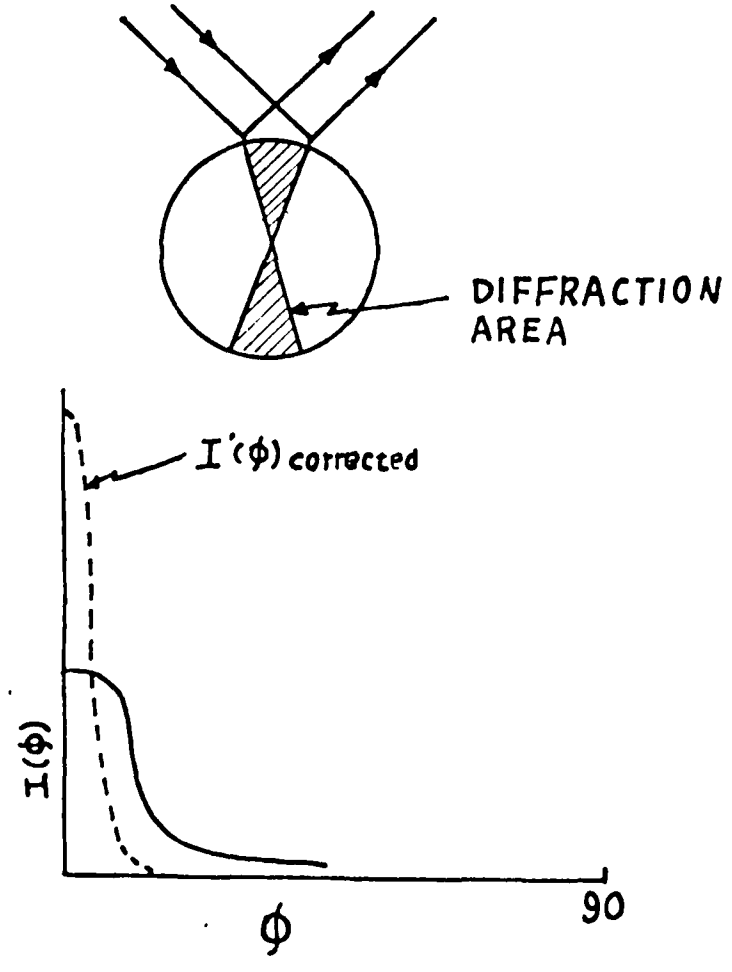

Schematic of small fractions diffracted by x-ray diffraction.

(B) Optical microscopy and preferred orientation

(1) Theory

Optical preferred orientation measurements can be made using three main techniques:

(i) Polarizer only

$$\frac{I_R}{I_O} = \frac{1}{2}(r^2 + s^2) + \frac{1}{2}(r^2 - s^2)\cos 2\theta$$

$$\frac{I_{MAX}}{I_{MIN}} = \frac{r^2}{s^2} \sim 2.8$$

Only a polarizer is used, and the sample itself behaves as the analyser. (r^2 and s^2 are the reflectivities parallel and perpendicular in the highest and lowest directions.) If the ratio of maximum light intensity to minimum is determined, the dependence on the incident light is eliminated. However, the range of I_{MAX}/I_{MIN} is only from 1 for isotropic to about 2.8 for fully oriented graphite. It is also insensitive to the high preferred orientations in fibers, but would be excellent for low preferred orientation materials.

The general case for a polarizer with an analyser at α is shown below:

$$\frac{I^2}{I_O} = \frac{1}{2}(r^2\cos^2\theta + s^2\sin^2\theta) + \frac{1}{2}\{(r^2\cos^2\theta - s^2\sin^2\theta)^2 + 4r^2 s^2 \cos^2(\gamma-\delta)\cos^2\theta\sin^2\theta\}^{\frac{1}{2}}\cos 2(\alpha-\alpha_o)$$

$$\tan 2\alpha_o = \frac{2rs\cos\theta\sin\theta}{r^2\cos^2\theta - s^2\sin^2\theta}\cos(\gamma-\delta)$$

(ii) Crossed polars

$$\frac{I}{I_0} = \frac{1}{8}\{r^2 + s^2 - 2rs\cos(\gamma-\delta)\}\cdot(1 - \cos 4\theta)$$

$$\frac{I_{MIN}}{I_0} = 0 \qquad \frac{I_{MAX}}{I_0} = .082$$

The sensitivity is higher, but incident intensity must be kept constant. Experimentally, the sample area and optics must also be kept constant, which is not convenient.

(iii) Apparent rotation angle "A_R"

The stage is rotated to give maximum light intensity with crossed polars (basal planes at 45° with respect to polarizer and analyser), Figure 8, and then the analyser is rotated to give minimum intensity, as shown in Figure 9. The value of the angle, A_R, at the minimum intensity describes the preferred orientation.

(2) Results using apparent rotation angle.

The value of the rotation angle at the minimum intensity describes the preferred orientation, Figure 10. Although the minimum is quite broad, the curve is a sin wave and can be evaluated by curve fitting all the experimental data. Incidentally, these measurements were determined with a photomultiplier limited to measuring light from a uniform small region. Earlier, visual estimates of A_R had been made with surprisingly similar results considering the broad minimum. However, the eye compares the local region of interest with the surroundings, and the effect the eye would generally see is shown in Figure 11.

$$\frac{I_{area}}{I_{surroundings}} \text{ vs. Analyser Angle}$$

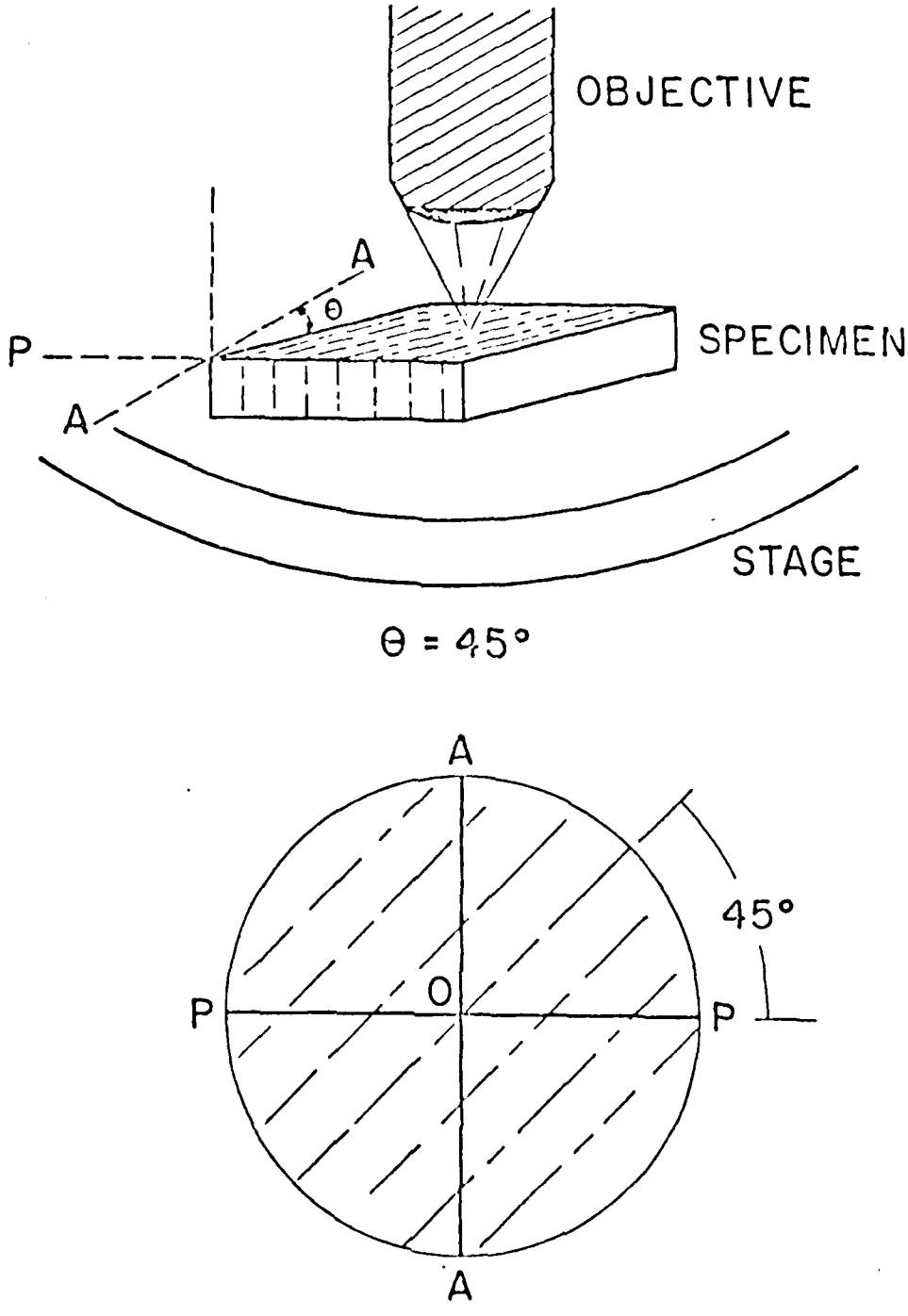

FIGURE 8: Schematic of specimen resting on microscope stage.

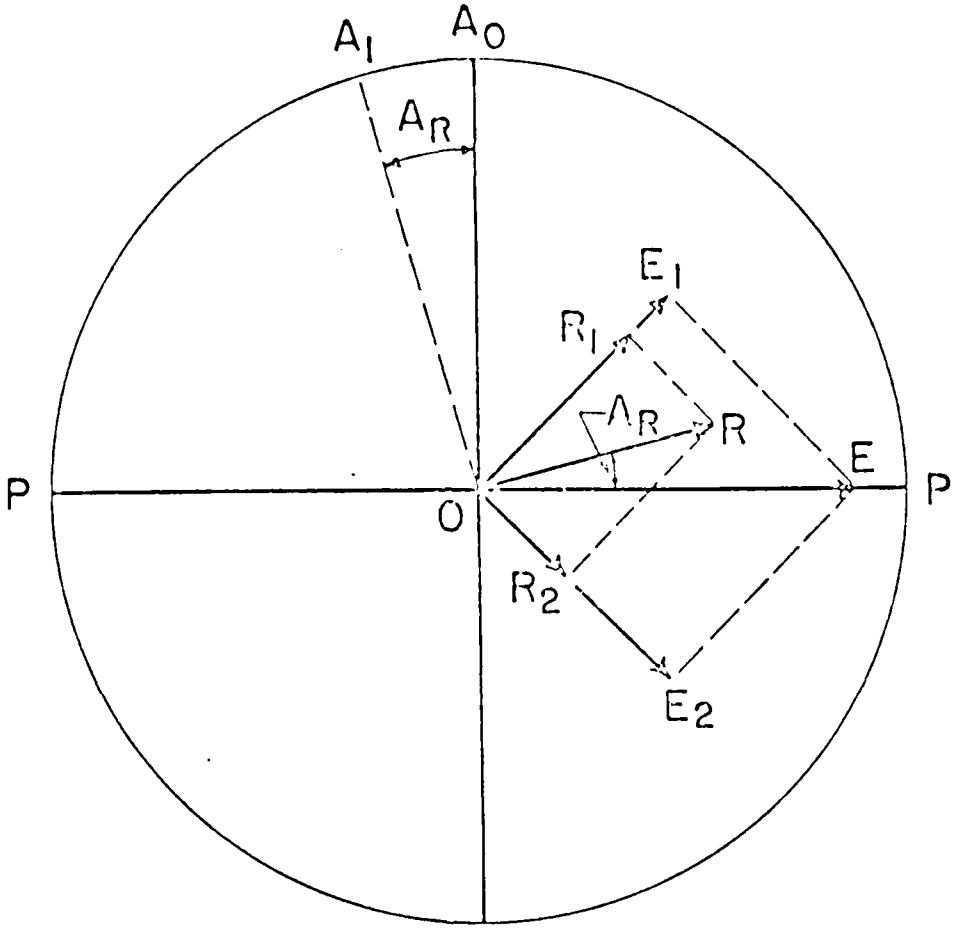

FIGURE 9: Vectorial light analysis diagram.

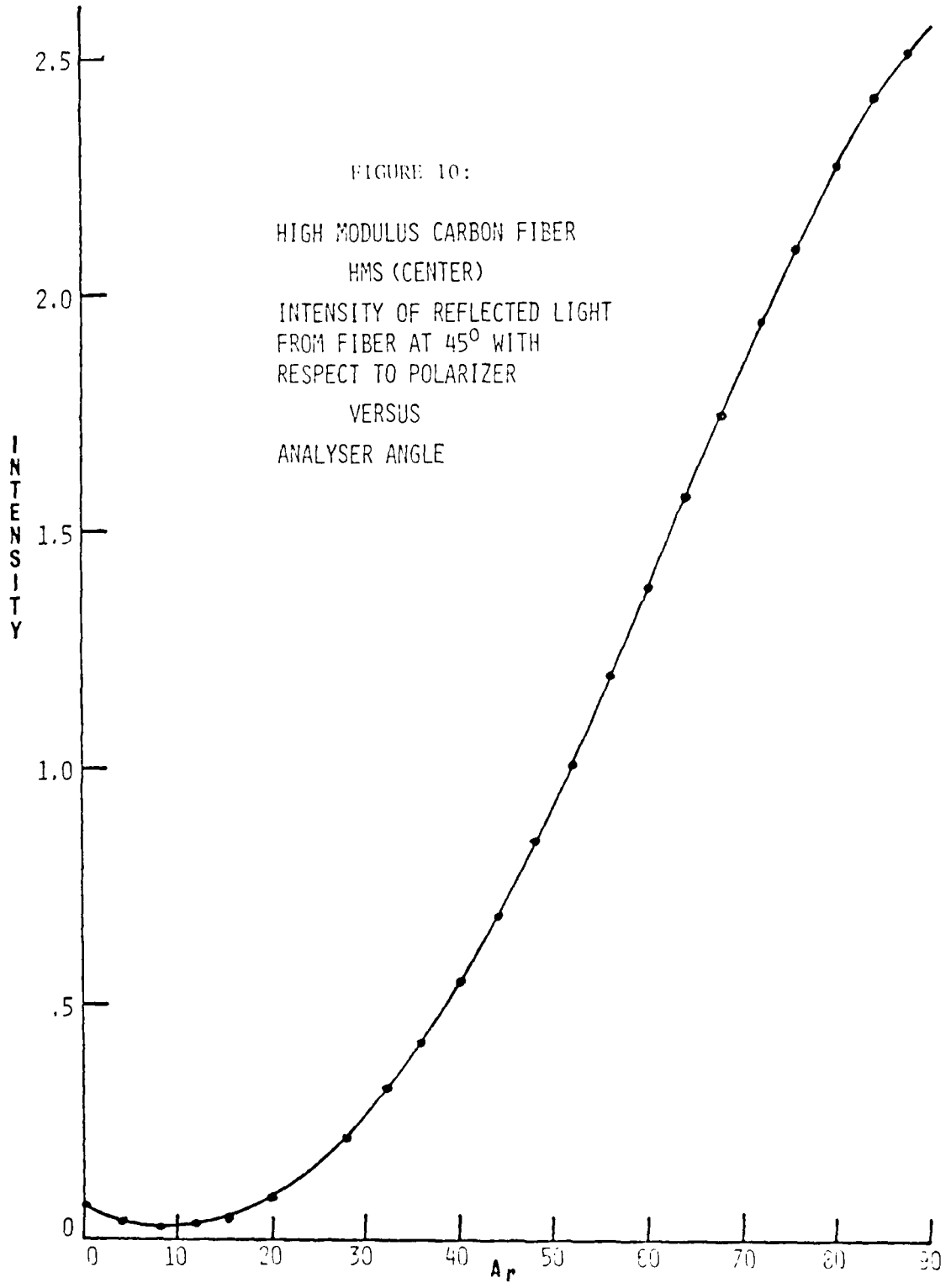

FIGURE 10:

HIGH MODULUS CARBON FIBER

HMS (CENTER)

INTENSITY OF REFLECTED LIGHT FROM FIBER AT 45° WITH RESPECT TO POLARIZER

VERSUS

ANALYSER ANGLE

FIGURE 11:

HIGH MODULUS CARBON FIBER (MI) CENTER

RATIO OF INTENSITY REFLECTED FROM FIBER AXIS AT 45° AND 0° WITH RESPECT TO POLARIZER VERSUS ANALYSER ANGLE

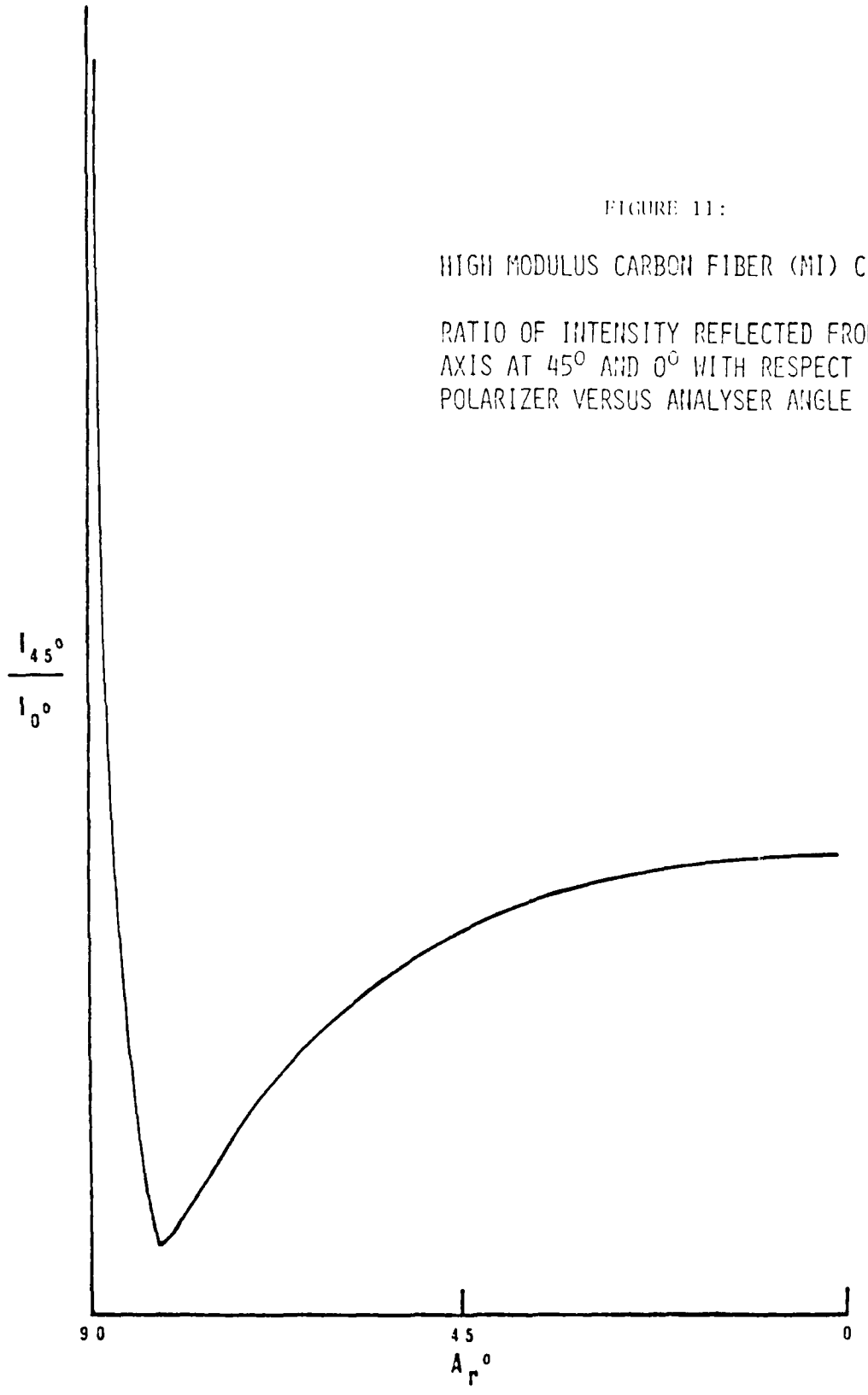

As can be seen for several high modulus fibers, the apparent minimum is sharp, and visual determinations of approximate rotation angles are precise.

(C) Comparison of preferred orientations determined by the x-ray diffraction and optical microscopy

A correlation between modulus and preferred orientation obtained from both the x-ray diffraction method and the optical microscopy method is shown in Figure 12. Both curves have the same trend, that is, the higher the preferred orientation (A_R or $\frac{1}{Z}$) the higher the modulus.

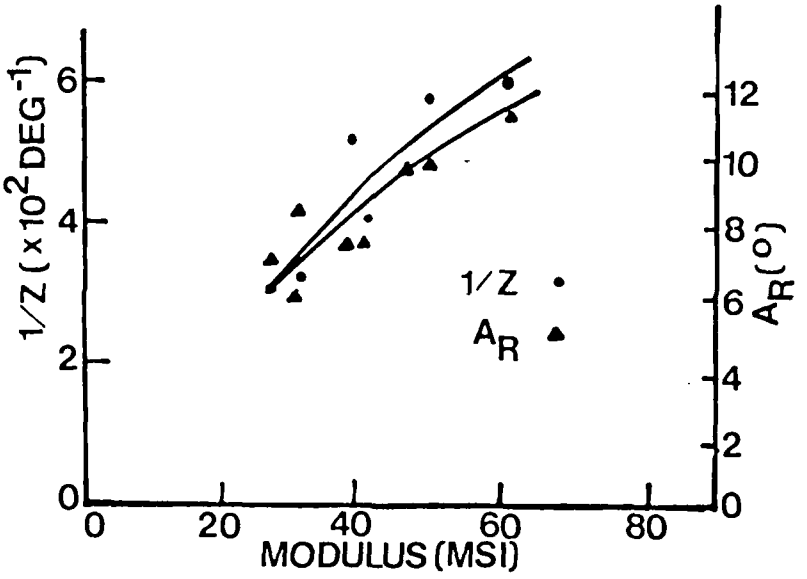

FIGURE 12

While the correlations for either method are not perfect, estimates of modulus could be made by either method.

(D) Residual stress

The optical activity observed in carbon fibers is a function of crystalline optical anisotropy and residual stress. The results described below were obtained to determine the importance of residual stress on optical measurements and also to access the effect residual stress might have on mechanical properties.

(1) Modulus vs. diameter relationship for as received carbon fibers

Figure 13 shows the relationship between modulus and HMS fiber diameters. Thin fibers apparently exhibit higher values of modulus than thick fibers. These results are similar to the work of Jones and Duncan[4].

(a) Error analysis of diameter measurement

(i) The diameters used in Figure 13 were measured from the edges of each fiber used in the tensile tests. A histogram is shown in Figure 14.

(ii) A bundle of fibers were mounted vertically in epoxy, then the diameter was measured with a fillar eyepiece (625X), Figure 15.
$\bar{X} = 7.81\mu$, $s = 0.31$, $n = 53$

(iii) The same sample used in (ii) was analyzed using a Bausch & Lomb FAS-2 Image analyser, Fig. 16, to count the corresponding diameter of each fiber. The histogram is shown in Figure 17.
$X = 7.74\mu$, $s_2 = 0.52$, $n = 53$

(iv) The diameter of a single HMS fiber was measured using a fillar eyepiece (625X) with random position rotation of the stage and fillar eyepiece viewer. A histogram is shown in Figure 18.
$\bar{X} = 8.25$, $s = 0.25$, $n = 55$

(v) The same sample as (iv) was observed with oil immersion (1562.5X). A histogram is shown in Figure 19.
$X = 8.37\mu$, $s = 0.11$, $n = 50$

(vi) The variance in (iv) is only determined by measurement errors while the variance in (ii) is a combination of both sample variance and measurement errors. Since the sample and measurement variances should be independent of

FIGURE 13

Modulus vs. diameter for original fibers.

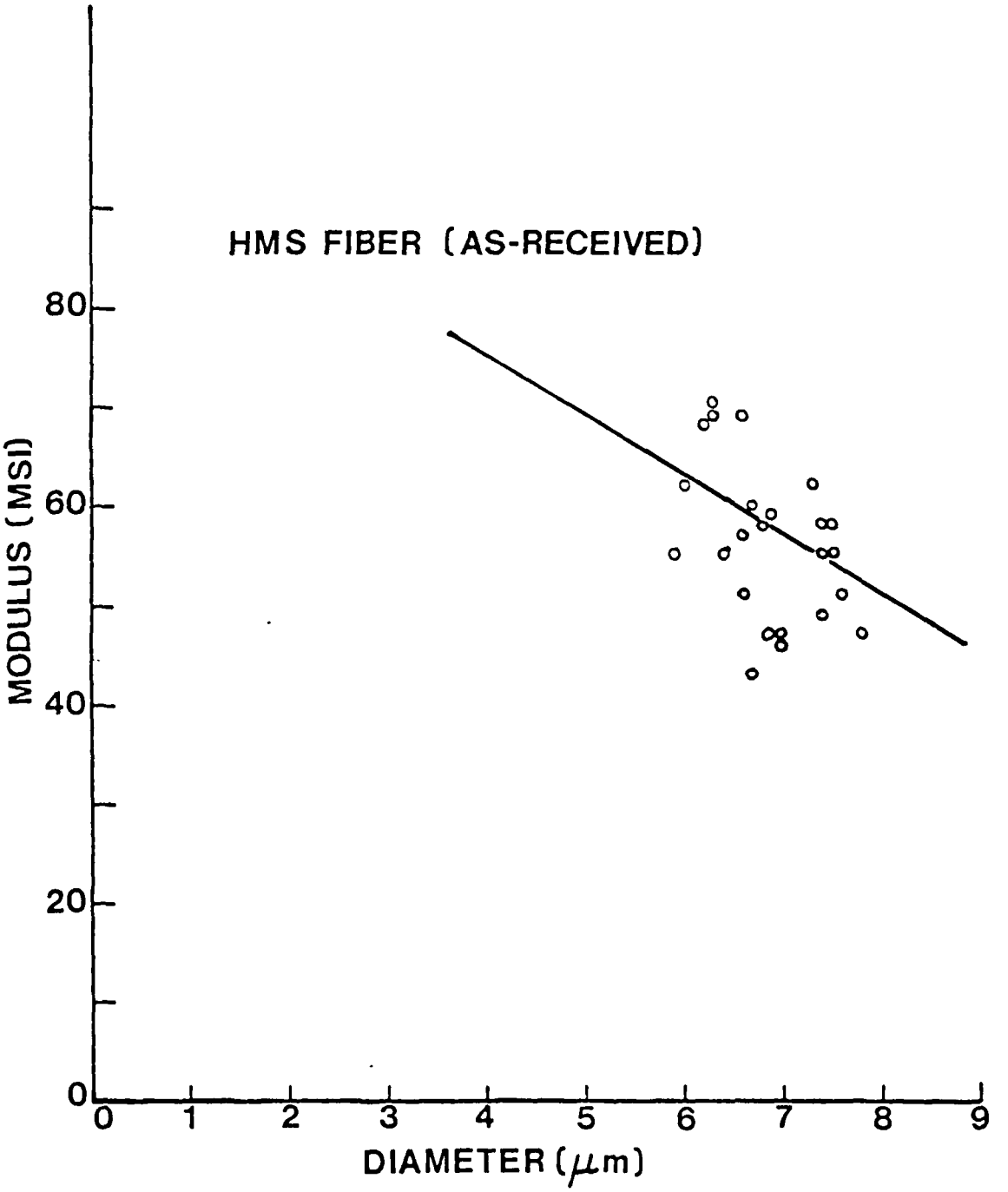

FIGURE 14:

Histogram of diameter for original fiber with edge.

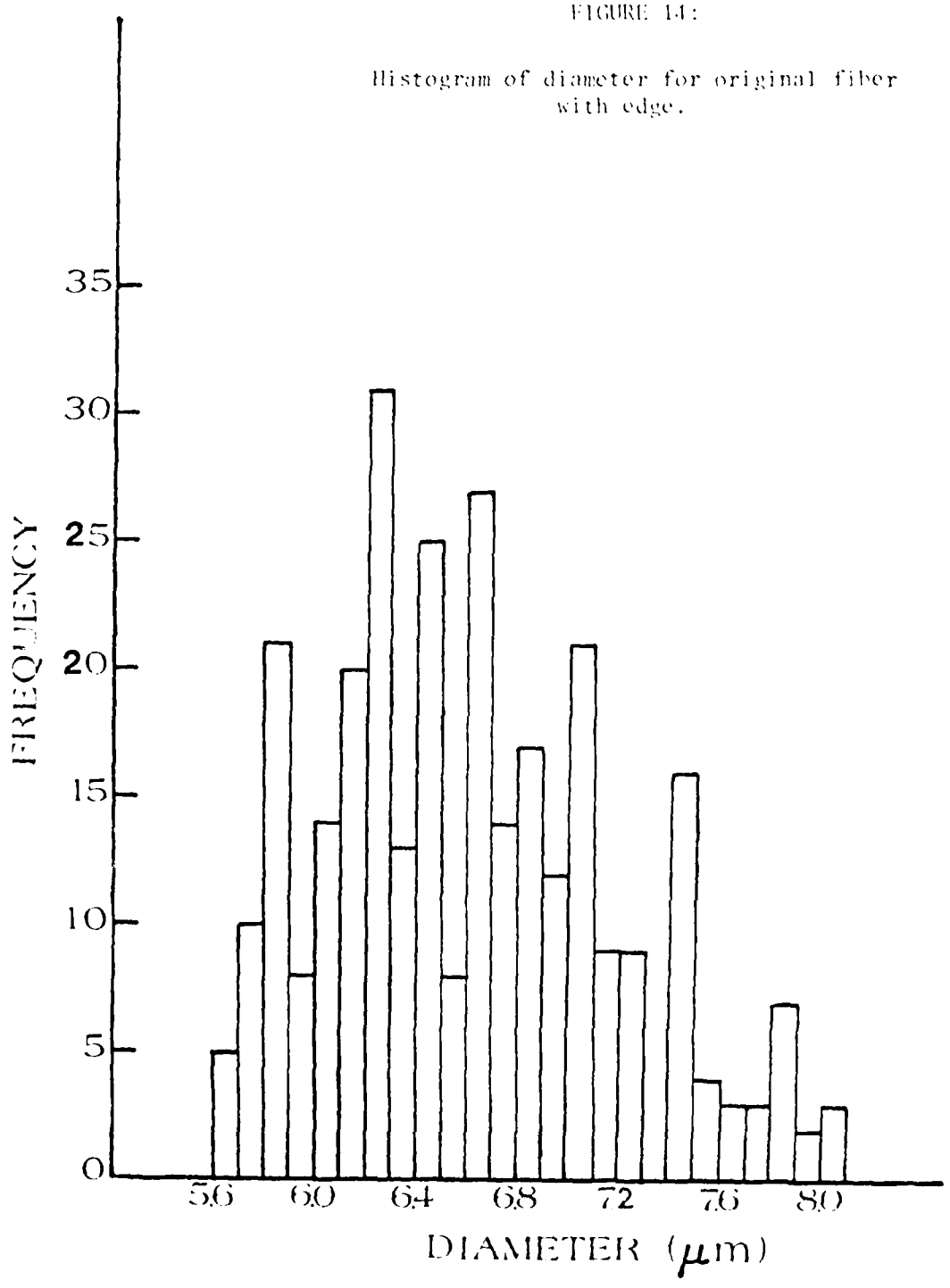

FIGURE 15:

Histogram of diameter for original fiber with cross-section (625X) fillar eyepiece.

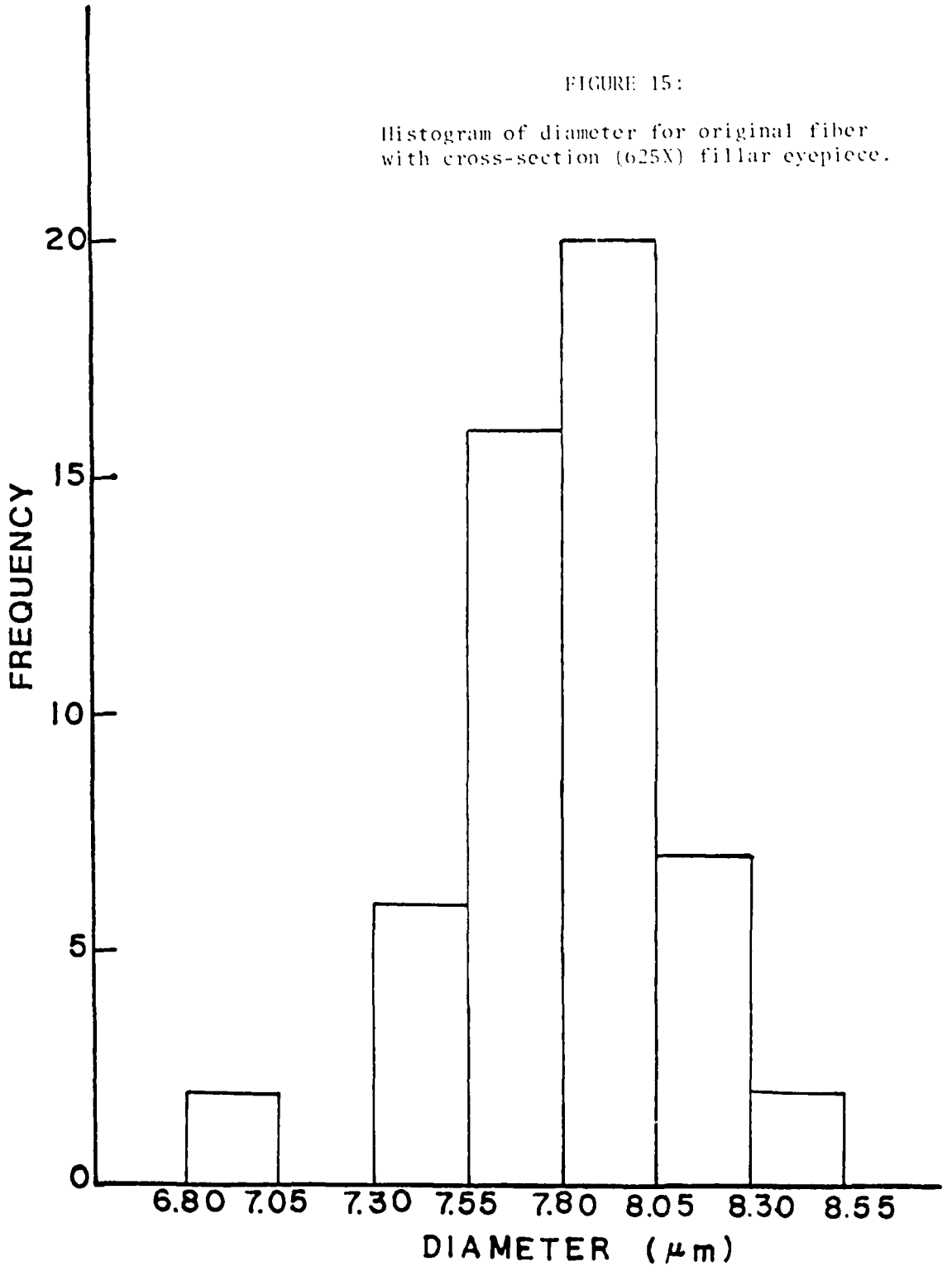

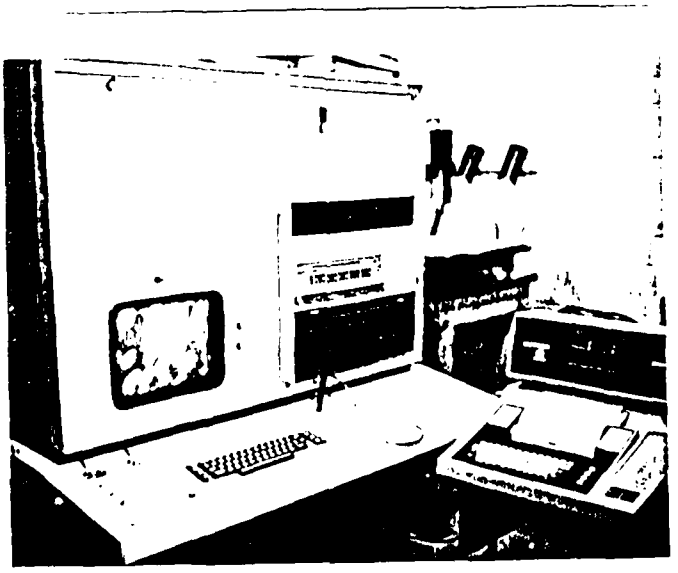

FIGURE 16: Image Analyzer System.

FIGURE 17:

Histogram of diameter for original fiber measured with Image Analyzer.

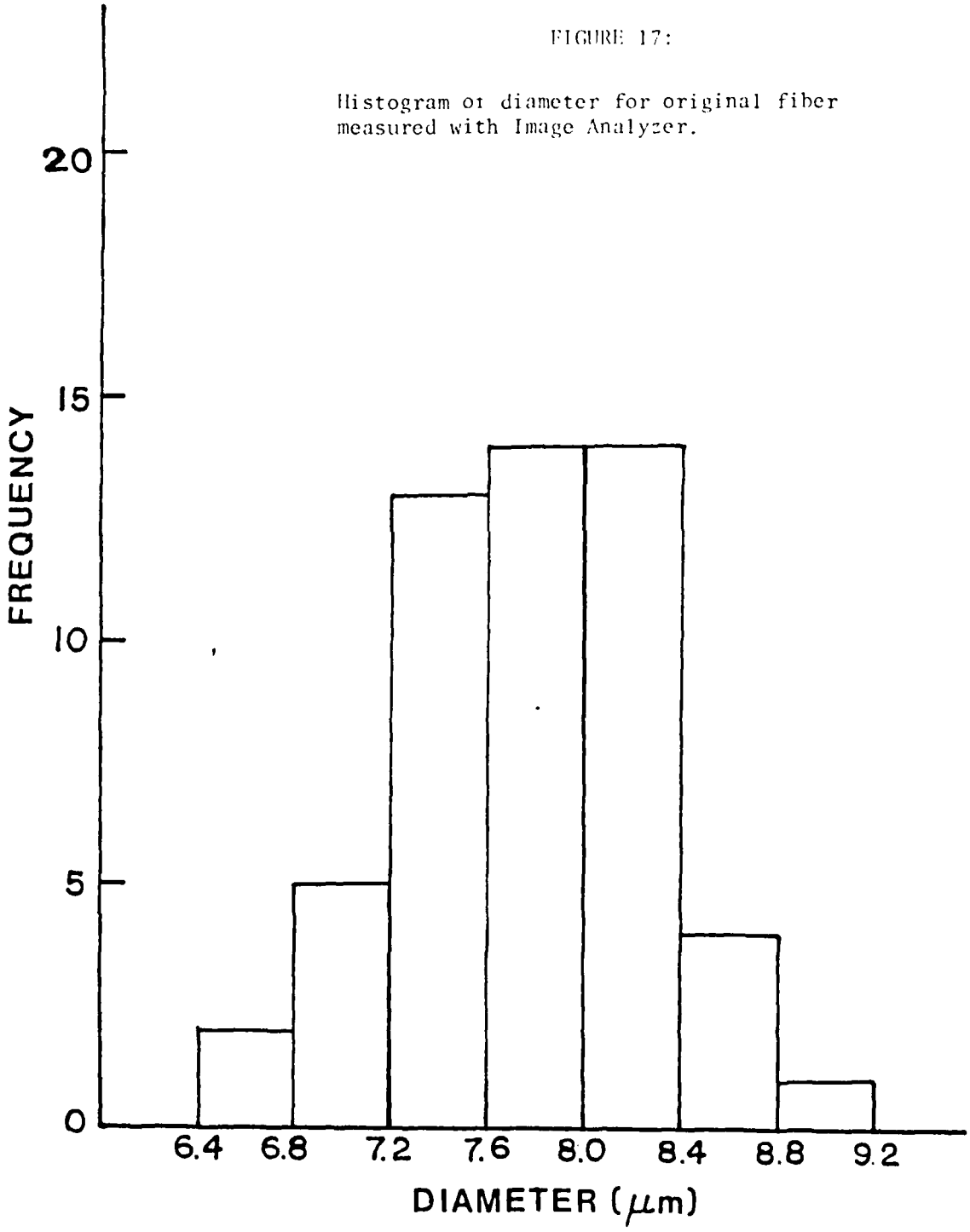

FIGURE 18:

Histogram of diameter of single fiber measured with cross-section (625X) fillar eyepiece.

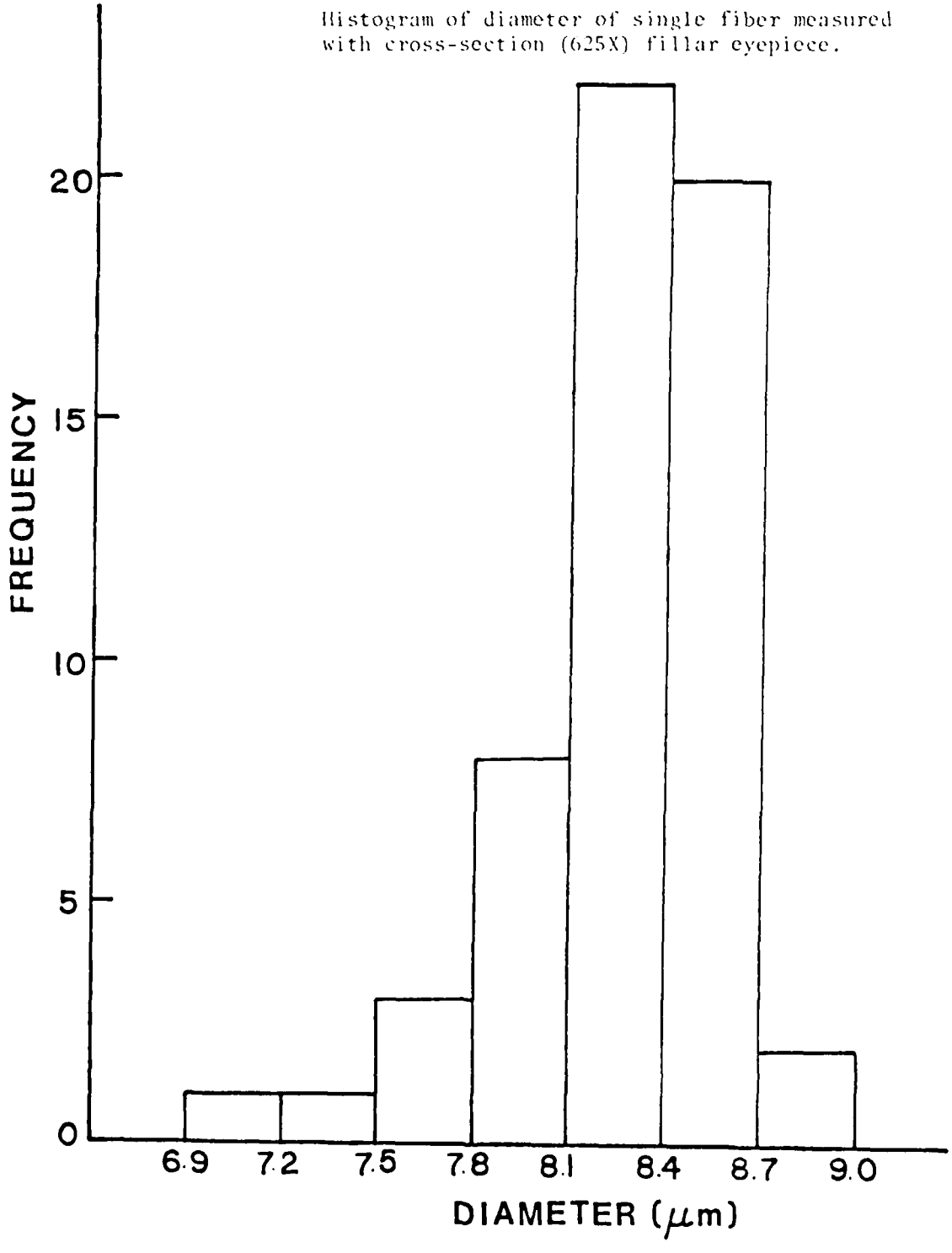

FIGURE 19:

Histogram of diameter of single fiber measured cross-section (1562.5) oil immersion.

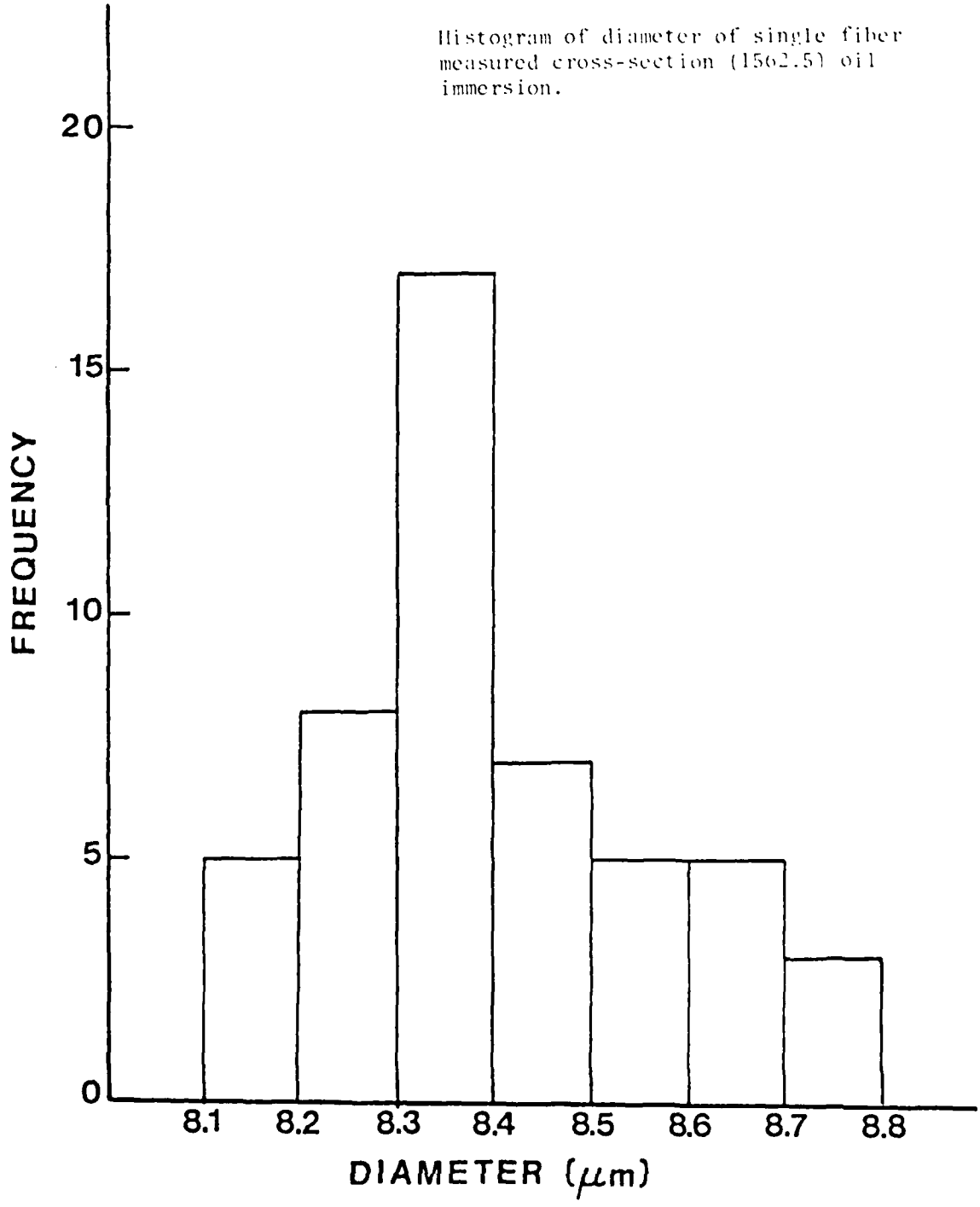

each other over the ranges studied:

$$S_o^2 = S_m^2 + S_s^2$$

where S_o^2 is the overall variance observed in (ii) or (iv)

S_m^2 variance due to measurement

S_s^2 variance due to samples

For case (iv), where the sample variance is zero:

$$S_o^2 = S_m^2 = .25^2$$

and substituting this estimate of variance into case (ii):

$$S_o^2 = S_m^2 + S_s^2$$

$$.31^2 = .25^2 + S_s^2$$

$$S = .18$$

Hence, the sample standard deviation is <u>less</u> than the standard deviation due to measurement errors.

The measurement deviations mainly consist of two parts which again are independent:

$$S_m^2 = S_r^2 + S_e^2$$

S_r = variance from reading the vernier

S_e = variance from setting the cross hair on the edge of fiber

Increasing the magnification will give larger differences in the vernier readings which decreases the value of S_r while S_e may stay constant. However, oil immersion increases contrast between fiber and matrix and improves resolution– so S_e decreases. Comparison of (iv) and (v) shows marked decrease in standard deviation in measurement errors when using an oil immersion objective at 1500X magnification.

Image analysis results (iii) had a much larger deviation of S = 0.52, but this was mainly caused by a low pixel count. Much higher magnification, to 5000X would decrease the standard deviation to about .2. This is not any better than direct optical measurement and also does not save time. Many times fiber diameters are measured by laying the fiber on its side. This would allow an average estimate of the width to be made from the area, and would be more accurate as the area is larger. However, the focus is critical as the fiber is not a planar surface. For filar measurements, the standard deviation was found to be significantly higher ($S \sim .45$), and more importantly, the average diameter was about 10% lower than determined by cross-sectional experiments. This average diameter difference is due to the fact that a focus error on the longitudinal fiber can be recorded as a smaller diameter. However, it should be realized that this error from measuring fiber diameters on their side results in an over-estimation of fiber strength and modulus of about 20%.

(b) Error analysis of slope measurement

A Bascom-Turner 8010 Recorder was connected to the tensile tester to plot σ versus ε. The same fiber was loaded 10 times, averaged, the curve smoothed and differentiated to get the slope of the σ-ε curve, i.e. modulus, as shown in Figure 20. There are two distinct slopes along the σ-ε curve.[5] Hence, care must be exercised to measure the same slope, when comparing different fibers. In particular, modulii would be significantly lower for lower strength fibers as the initial modulus would be emphasized. The correlation between strength and modulus for fibers obtained from a single batch may be artifact because of this effect and a common fiber diameter measurement error.

FIGURE 20: Two slopes in stress-strain curve.

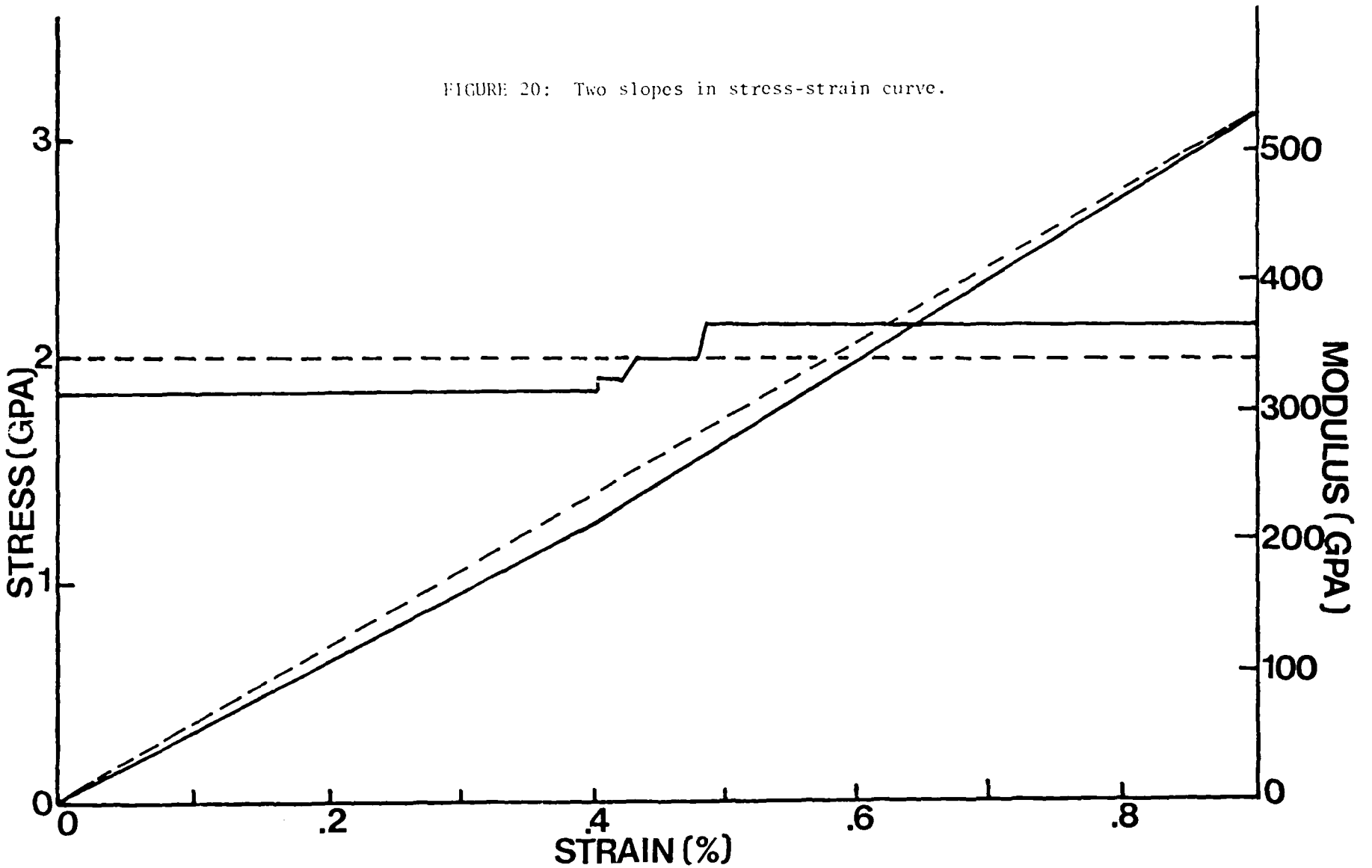

(c) Thought experiment: measurement errors and modulus or strength/diameter relationships.

(i) Suppose we have a tow of fibers with constant diameter and constant modulus fibers. What effect would measurement errors in diameter give? From the error analysis, it is known that even with the oil immersion method at 1500X, the standard deviation is 0.1, that is about 70% of the fibers will have $\pm$ 0.1 error in diameter. This error in diameter measurement is enough to produce a trend in modulus vs. diameter plots, i.e., the smaller the diameter, the larger the modulus. If the fiber diameters are allowed to vary, and the estimates of fiber diameter standard deviation and measurement standard deviation are used from section IIID(1)(a)(vi), the trend of observed modulus versus diameter (area) for Fortifil 5Y (also Courtelle PAN precursor) is correctly predicted assuming a constant modulus for all fibers, Fig. 21.

(2) Modulus vs. diameter for air-oxidized fibers

Bundles of fibers were oxidized in air at different temperatures for various periods of time. The fibers were examined using SEM for uniformity of oxidation. Although the etching was observed to be non-uniform for some times and temperatures, results of modulus vs. diameter are shown in Figure 22 for all groups of fibers oxidized. While each group showed an increase in modulus with decreasing diameter, the group average modulus decreased with decreasing diameter. Hence, as the average diameter becomes smaller as the oxidation time increases the smaller the modulus becomes. Therefore, a modulus gradient exists with the outside of the fiber having a higher modulus than the inside of the fiber. Although the

FIGURE 21

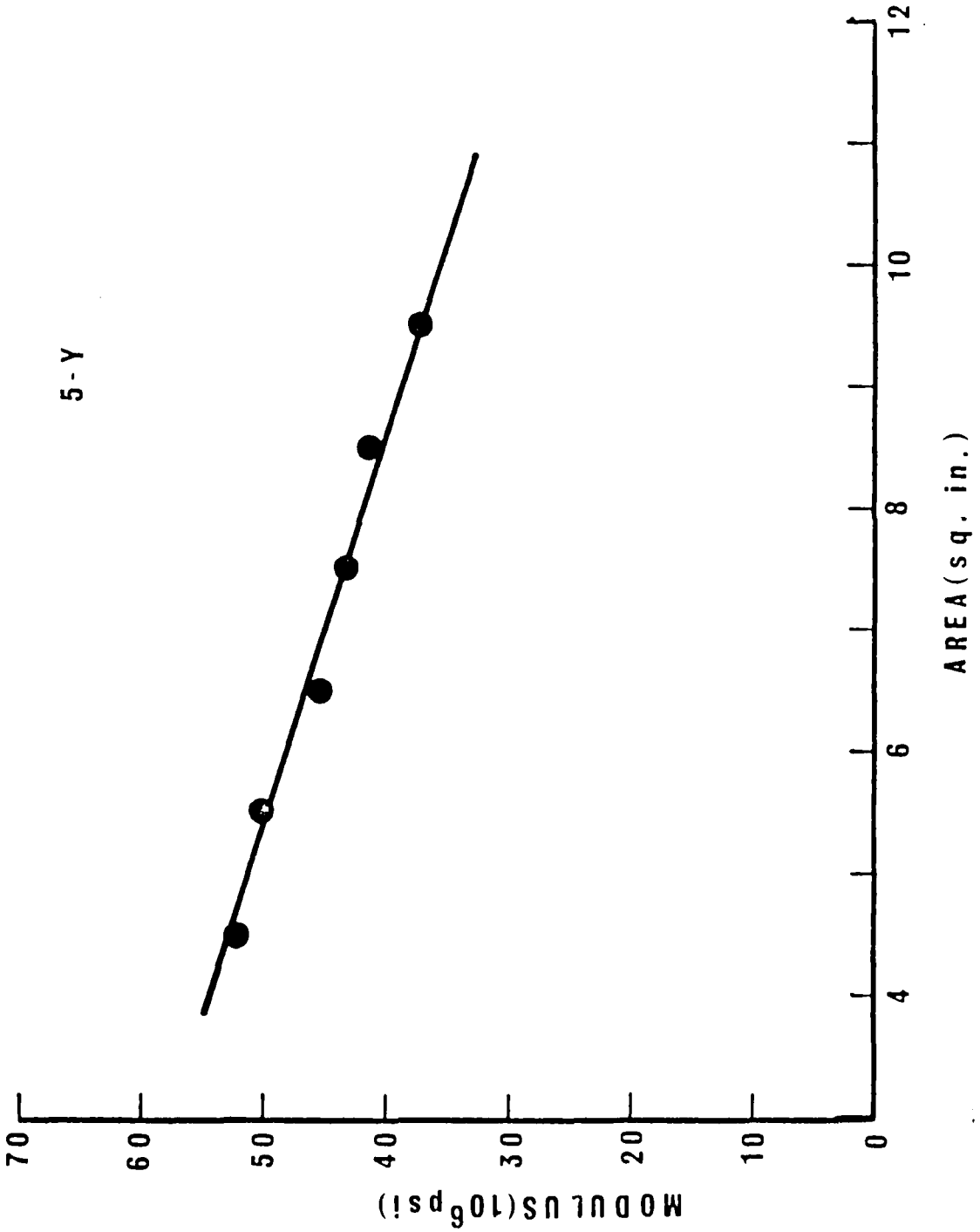

FIGURE 22: Modulus vs. diameter for oxidized fibers.

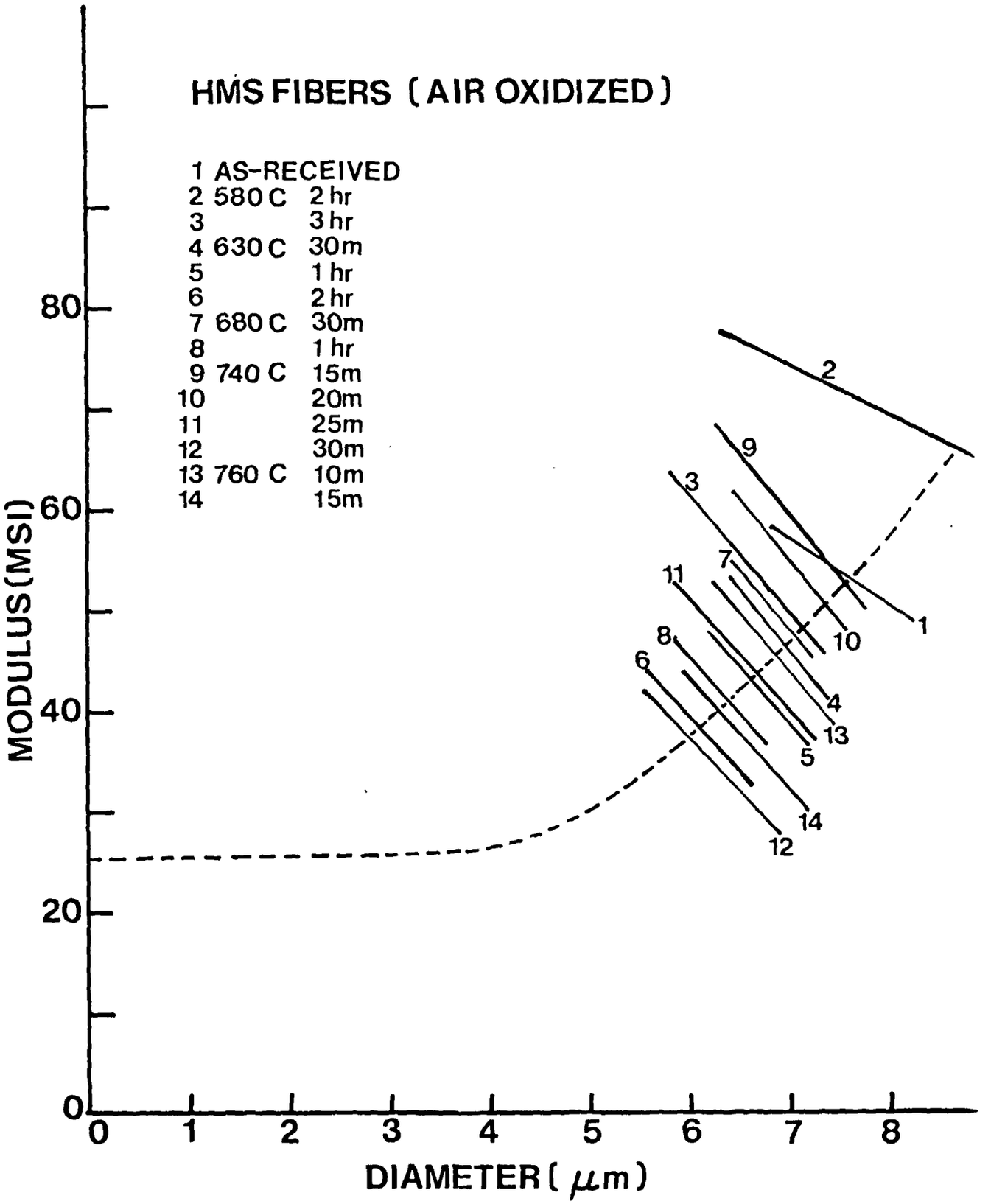

scatter is high for this raw data, it can be significantly reduced. If by chance the diameters of fibers selected for mechanical testing are smaller than the bundle average, the observed modulus will be high. By assuming an average slope exists for modulus versus diameter within a group, the modulus can be normalized for the true average diameter.

(3) Strain results

Using ion sputtering to thin fibers, the contraction of fibers was measured using SEM (Figure 23). An unmeasured error, which involves the ellipticity in fiber cross-section and which may develop with ion thinning, may affect the accuracy of this experiment. Nevertheless, the fiber is observed to contract as the outer surface is sputtered away.

(4) Residual stress

Once the local modulus and local strain have been established, the residual stress within carbon fibers is the product of modulus and strain at each location within the fiber (Figure 24). Details on calculations for converting average modulii and strains to local modulii and strains is covered in Reference 6. The calculated compressive stress at the surface is very high. Although the actual magnitude of the residual stress may be significantly in error because of the strain measurements, especially near the fiber surface, the fiber does appear to have sufficiently high residual stresses to affect fiber strength.

IV. CONCLUSIONS

(1) Preferred Orientation either expressed by $W_{\frac{1}{2}}$ or A_R can be related to axial properties of fibers. For no matter what kind of fibers, the higher the preferred orientation, the higher the modulus.

(2) Many correlations between properties and fiber diameter reported in the past may be in error because it is very difficult to determine the

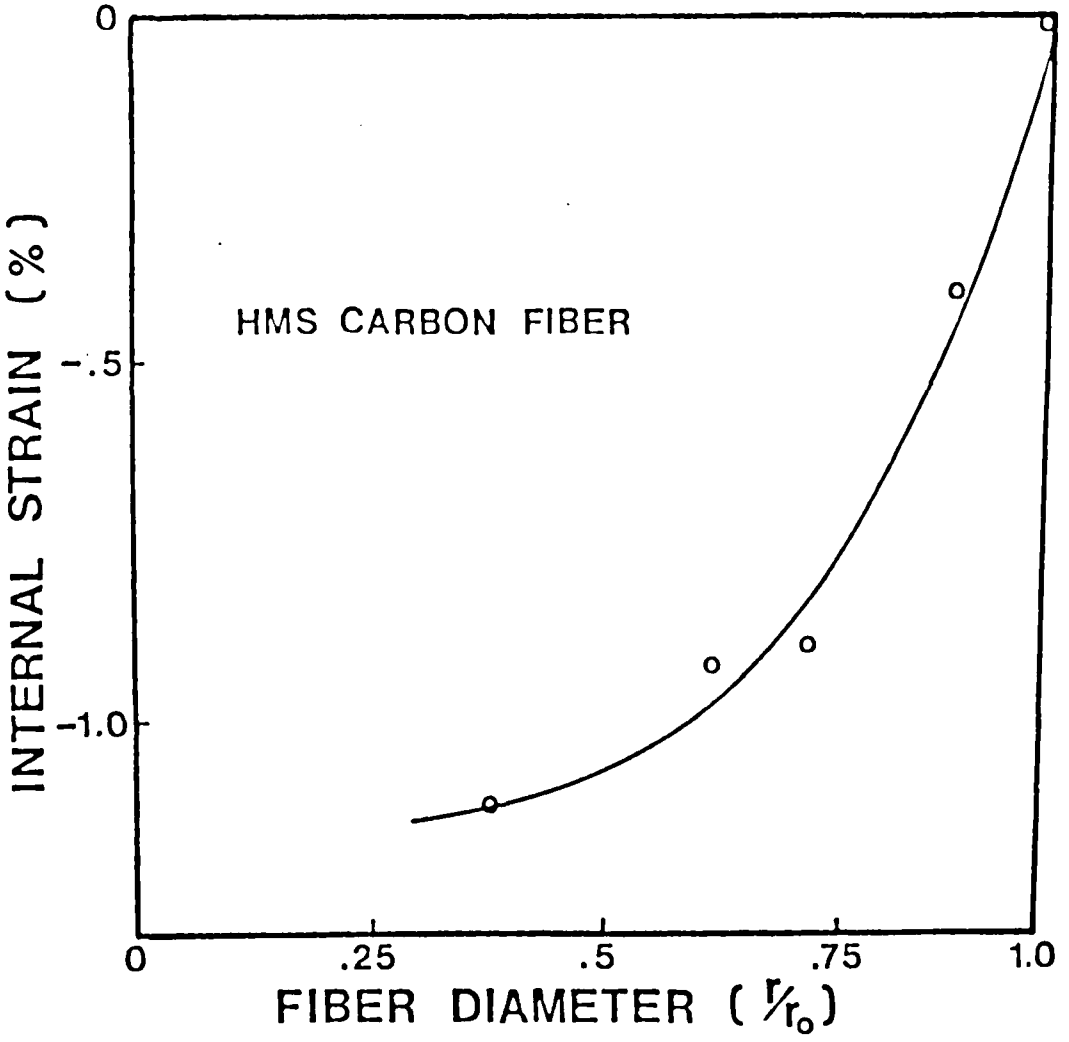

FIGURE 23 - Contraction of a HMS carbon fiber as a function of etched fiber radius. Surface layers were removed by ion thinning.

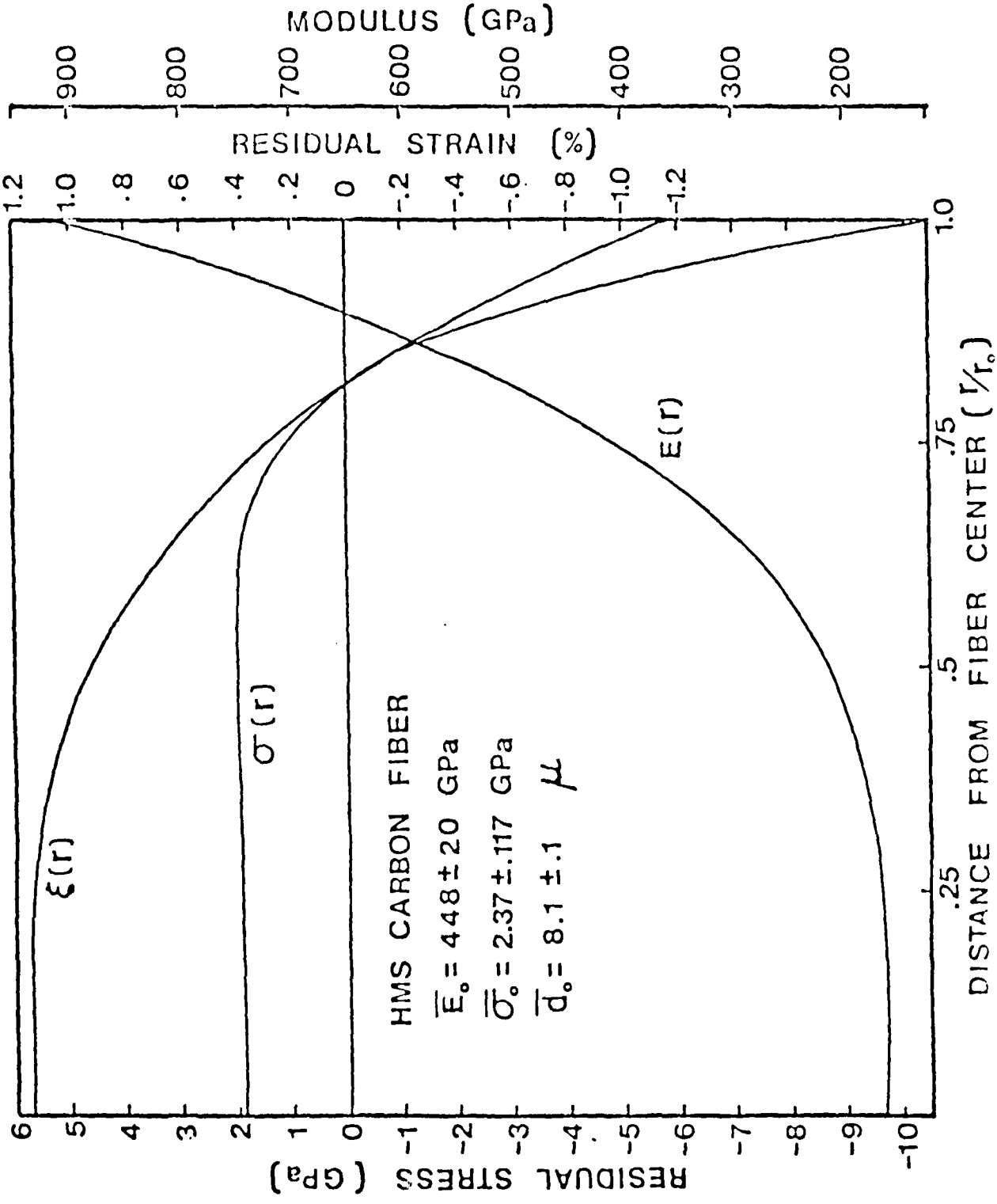

FIGURE 24 - Axial modulus strain and stress profiles of HMS carbon fiber.

diameter of the fiber accurately.

(3) The small effect of surface abrasion on the strength of high modulus carbon fibers suggests compressive axial residual stresses at the fiber surface. This was confirmed by finding high residual stresses in HMS fiber.

(4) For a high modulus PAN precursor fiber (Hercules HMS), the modulus was found to be significantly higher at the fiber surface than in the center.

REFERENCES

1. Bacon, G. E., "Method for Determination of Degree of Orientation of Graphite", J. Appl. Chem., 6, 477, Nov. (1956).

2. Ruland, W., "X-ray Studies of Preferred Orientation in Carbon Fibers", J. Appl. Physics, 38, 3585, (1967).

3. Butler, B. L., "The Effects of Carbon Fiber Microstructures on the Shear Strength of Carbon Epoxy Composites", Ph.D. Thesis, RPI, (1969).

4. Jones, B. F., and Duncan, R. G., "The Effect of Fiber Diameter on the Mechanical Properties of Graphite Fibers Manufactured From Polyacrylonitrile and Rayon", J. Mat. Sci., 6, 289, (1971).

5. Curtis, G. J., Milne, J. M., and Reynolds, W. N., "Non-Hookian Behavior of Strong Carbon Fibers", Nature, Vol. 220, 1024, (1968).

6. Stevens, W. C., Wang, J. H. and Diefendorf, R. J., "Residual Stress in High Modulus Carbon Fibers", Carbon '80, pp. 598-602, Deutchen Keramischen Gesellschaft, Bad Honnef, W. Germany.

RESIDUAL STRESS IN HIGH MODULUS CARBON FIBERS

W. C. Stevens, J. H. Wang* and R. J. Diefendorf
Rensselaer Polytechnic Institute, Troy, New York, 12181, U.S.A.

Microstructural studies and the small effect of surface abrasion on the strength of carbon fibers suggest compressive residual stresses at the fiber surface. A qualitative confirmation of these stresses was obtained by noting fiber curvature when one side of a high modulus carbon fiber was ion milled away. Quantitative data on residual stresses were calculated from modulus and residual strain distributions, which were obtained by selectively oxidizing fibers to different diameters. The magnitude of the axial compressive residual stress at the surface of HMS fiber is several GPA.

Residual stress, fibers, modulus gradient.

Introduction

Transmission electron microscopy of carbon fibers reveals an undulating ribbon microstructure with high axial alignment of the ribbons near the surface and a lower alignment toward the fiber's center because of higher amplitude ribbon undulations.[1,2,3,4,5] (Figure 1.) This change in the amplitude/wavelength ratio of the ribbons results in a modulus gradient within the fiber with the surface layers having a higher modulus and the core material a lower modulus.[6] The variation in axial preferred orientation also results in a gradient in the coefficient of thermal expansion across the fiber's transverse section.[7] Since the CTE of the basal plane is lower than that transverse to the basal plane, it is expected that the fiber's interior, having a larger component of the transverse properties, has a higher CTE. The varying CTE places the restrained interior into tension and the outer layers under compression upon cooling from processing temperatures. This compressive stress at the surface may account for the insensitiveness of carbon fibers to surface flaws.[8,9,10,11,12] During cooling from processing temperatures, radial and hoop residual stresses also develop within carbon fibers due to transverse preferred orientation in these fibers.[7] These residual stresses can cause cracks to develop parallel to the fiber axis which degrades fiber strength.[13]

This paper will discuss various techniques developed to characterize microproperties and to determine the axial residual stress in carbon fibers.

Experimental Techniques

The surface layers of carbon fibers were successively removed by gaseous oxidation, wet oxidation, or ion milling. For air oxidation, the fibers were cleaned with HCl, then dried and placed into a furnace at 650°C. Wet oxidation was carried out by placing the fibers in a solution of 500ml concentrated H_2SO_4, 450ml of concentrated HNO_3 with 5gm of dissolved sodium dichromate at 65°C. Fibers to be ion thinned were mounted onto a metal washer which was fastened to the stage of the sputtering apparatus. The stage rotated between two opposed sputtering guns operating at 6000v and 50ua which permitted more uniform sputtering of the fibers. The fibers in all three cases were thinned to different reduced diameters by varying the lengths of furnace or sputtering time.

Fiber strain and diameter measurements were made with either an optical or with a scanning electron microscope. A square reference grid was photographed with the fiber when using SEM to correct for asymmetrical distortion and to reduce magnification errors. Both the stiffness and the fracture load of carbon fibers were measured with a fiber tensile tester. Fibers (2.5cm gauge length) were mounted individually and a segment of the fiber was saved for diameter measurement. A compliance correction for the tensile tester was used in the modulus determinations.

A technique was developed to measure contraction of fiber segments less than 0.5cm in length. A reference fiber was mounted straight and a specimen fiber was mounted in a circular arc on a washer as shown in Figure 2a. Both fibers were then sputtered and the contraction of the specimen fiber was measured, Figure 2b. As compressive surface layers were removed during sputtering, the fiber shrank. The straight reference fiber naturally remained stationary; however, the arced fiber drew away from the reference fiber as the arced fiber contracted. The measurement of separation distance between the reference fiber and the arced fiber was an indirect measurement of the residual stress of the specimen fiber. The calculation is shown in Appendix I.

*Now with I.B.M., East Fishkill, New York, U.S.A.

Results and Discussion

A) Evidence of Axial Residual Stress and Its Origin

Commercially available carbon fibers in free state are straight and residual stresses within the fibers must be balanced. But if the surface layer on just one side of a fiber is ion milled away, the stresses within the straight fiber will no longer be balanced; the moment that is created will cause the fiber to curl and seek a state where the net moment is again zero. When outer layers of one side of a carbon fiber were sputtered off, the fiber curled in the direction of the ion gun indicating that the surface layers were under compression.

The origin of residual stresses is postulated to predominantly arise from the transverse gradient in the axial CTE of the fiber and arises during the cooling from final processing temperature. This hypothesis was supported in the following experiment. Curled fibers, which had been produced by sputtering away one side only of a fiber, were heated and observed to partially straighten. If the curl was due to differential contraction produced on cooling from the graphitization temperature, the differential strain within the fibers upon heating should decrease which would result in a straightening of the curled fibers.

B) Modulus and Strength Gradient

Both the modulus and the strength of HMS fibers decreased after the outer layers of these fibers were removed. (Figure 3.) Because of experimental difficulties, modulus and strength at the center of Hercules HMS fibers are unknown. As the fibers were reduced in diameter, handling of these delicate fibers became a difficult problem. Standard tensile tests were unreliable for fibers with diameters less than 4 microns due to the low fracture load of the fibers. For each batch of fibers tested, a distribution in diameter, modulus, and strength was measured. Generally smaller diameter fibers within a batch tend to possess higher strength and modulus while larger diameter fibers have lower modulus and strength.

1) Modulus Gradient

The form of the equation for describing the modulus was selected by requiring that the modulus be continuous, smooth, emit an unique derivative ($r = 0$), and be consistent with microstructural observations. From these assumptions, a best fitting fourth power function, $Y(r)$, was calculated by regression analysis using all the individual points. The function $Y(r)$ is the average modulus (GPA) of reduced area HMS fibers with radius r measured in microns.

$$Y(r) = 166 + .929r^4 \qquad (1)$$

If a weighted regression analysis, using the group average, is used:

$$Y(r) = 129 + 1.15r^4 \qquad (2)$$

The difference between the two equations is caused by the magnified effect of outlying points when the individual points are used. Although the group average regression constants give a better visual fit when the group average points, the individual point regression constants were used in later calculations to more accurately describe the raw data.

From the average modulus function $Y(r)$, the local modulus $E(r)$ at radius r, can be calculated (Figure 4) by:

$$E(r) = Y(r) + \frac{r}{2}\,\frac{dY(r)}{dr} \qquad (3)$$

The calculated modulus is high at the surface of HMS fibers and then decreases quickly for the less aligned material toward the center of the fiber.

The origin of the modulus gradient probably relates to relaxation during the initial stabilization stage of carbon fiber processing (of the oriented PAN precursor fiber). Highly aligned molecules produced during stretching of the precursor remain aligned only at the surface because of rapid cyclization. However, molecules near the center of the fiber stabilize more slowly due to a decreased oxygen concentration and are more apt to relax and subsequently form a more poorly aligned structure at the interior of carbon fiber. The alignment at the surface is retained through the carbonization process to produce high modulus at the surface of the carbon fiber, while the more poorly aligned interior results in lower modulus.

2) Strength of Oxidized Fibers

When the compressive surface layers of carbon fibers were removed, the average strength of these fibers decreased. Since the high surface compressive stress was removed, the mechanism which helps to reduce the initiation and propagation of flaws at the surface is no longer present. This supports the thesis that compressive residual stress strengthens HMS carbon fibers. The sharp reduction of measured strength would indicate that the magnitude of residual stress within carbon fibers is high or the outer part of the fiber is the highest strength portion of the fiber.

3) Strain Gradient

The contraction measurement of carbon fibers proved difficult. Contractions are small and ion sputtering data showed variations among measurements. Measured contractions, e(r), are the equilibrium rest positions of a fiber after surface layers greater than distance r from the center of the fiber have been removed. The contractions, e(r), are different from the local strains, ε(r), of material at distance r from the axis of the fiber. By considering the balance of forces, the measured contractions, e(r), can be transformed into local strains, ε(r), with:

$$\varepsilon(r) = e(r) + \frac{de(r)}{dr} \frac{\int_0^r rE(r)dr}{rE(r)} \qquad (4)$$

A fourth order polynomial was used to fit the data with the following function resulting:

$$e(r) = -.01145 + 1.16*10^{-5}r^2 + 4.44*10^{-9}r^4 \qquad (5)$$

From the approximate function e(r), the local strain profiles, ε(r), within carbon fibers were calculated. (Figure 4.)

4) Residual Stress Gradient

Once the local modulus, E(r), and the local residual strain, ε(r), have been established, the residual stress within carbon fibers is the product of modulus and strain at each location within the fiber (Figure 4).

The calculated compressive stress at the surface is very high. Although the actual magnitude of the residual stress may be significantly in error because of the strain measurements*, especially near the fiber surface, the fibers do appear to have sufficiently high residual stresses to affect fiber strength.

5) Consequences on Fiber Properties

While high surface compression minimizes the effect of surface flaws,[10] the high axial tensile stress in the interior may decrease strength by causing fracture to initiate at flaws in the interior rather than at the surface. Similarly, the high axial compressive stressed outer layers of a fiber may initiate buckling when the fiber is compressively loaded. Modifications of the residual stress pattern might allow increased tensile and/or compressive strengths to be obtained in high modulus carbon fibers. A modulus gradient also exists within carbon fibers. The modulus of the surface layers is about twice the average fiber modulus while the interior modulus is only about one-half the average. This modulus gradient suggests that higher modulus carbon fibers could be produced if the modulus at the interior of these fibers could be increased.

Conclusions

All evidence indicates the existence of axial residual stresses in high modulus HMS carbon fibers. The curled fiber experiment, the resistance of fibers to strength degrading surface treatments, the contraction of fibers after the removal of their surface layers, and the residual strain gradient derived from an understanding of the internal structure of carbon fibers all support the conclusion that the surface layers are in axial compression and the center of these fibers are in axial tension. These residual stresses appear to be large and should affect fiber strengths.

*Critical fiber contraction measurements will be performed for fibers with just thin layers of surface removed. The magnitude of the axial compressive residual stress at the outer surface can then be estimated by:

$$\sigma_{surface} = \frac{r E_{avg}}{2} \frac{de(r)}{dr}$$

REFERENCES

1. D. J. Johnson and C. N. Tyson, "The Fine Structure of Graphitized Fibers", Brit. J. Appl. Phys. (J. Phys. D.) 2, 787 (1969).
2. A. Fourdeux, C. Herinckx, R. Perret, and W. Ruland, "La Structure des Fibres de Carbone", C. R. Acad. Ser., 269, 1597 (1969).
3. J. A. Hugo, V. A. Phillips, and B. W. Roberts, "Intimate Structure of High Modulus Carbon Fibers", Nature, 226, 144 (1970).
4. E. W. Tokarsky, "The Relationships of Structure to Properties in Carbon Fibers", Ph.D. Thesis, Rensselaer Polytechnic Institute, October 1973.
5. E. V. Murphy and B. F. Jones, "Surface Flaws on Carbon Fibers", Carbon 9, 91 (1971).
6. J. W. Jones and D. J. Thorne, "Effect of Internal Polymer Flaws on Strength of Carbon Fibers", Carbon 7, 659-661 (1969).
7. N. Tyson, "Fracture Mechanism in PAN Fibers 1000-2800C", Applied Physics 8, 749-758 May 11, 1975.
8. D. M. Riggs, I. W. Sorensen, and R. J. Diefendorf, "The Relationships of Structure to Properties in Graphite Fibers", AFML-TR-72Y33 Part IV, Nov. 1975.
9. R. M. Mehalso, "CVD of Boron on Carbon Monofilament", Ph.D. Thesis, Rensselaer Polytechnic Institute, November 1973.
10. W. R. Jones and J. W. Johnson, "Intrinsic Strength and Non-Hookean Behavior of Carbon Fibers", Carbon 9, 645-655 (1971).

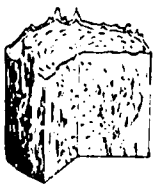

FIG. 1

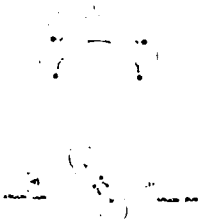

FIG. 2

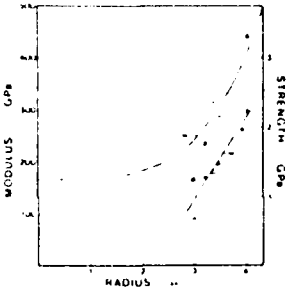

FIG. 3

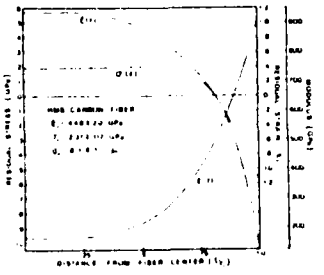

FIG. 4

FIG. 5

FIG. 1 - Schematic microstructure of HMS PAN carbon fiber.
FIG. 2 - Measurement technique of fiber contraction as a result of ion milling surface layers away.
FIG. 3 - Average modulus and strength vs. radius after the removal of successive surface layers.
FIG. 4 - Axial modulus strain and stress profiles of HMS carbon fiber.
FIG. 5 - Strain determination of ion milled carbon fibers.

APPENDIX I - Calculation of Fiber Strain From Contraction Experiment.

Arced fibers are portions of circles (Fig. 5) described by: $x^2 + y^2 - R^2 = 0$. The length of the arced, unetched fiber is $L_A = 2\theta_A R_A$ where

$$R_A = \frac{d^2 + h^2}{2h} \quad \text{and} \quad \theta_A = \sin^{-1}\left(\frac{d}{R_A}\right)$$ in radius. When the etched fiber contracts to circle B the length can be calculated similarly. The fiber strain is

$$\epsilon = \frac{\Delta L}{L} = \frac{2\theta_A R_A - 2\theta_B R_B}{2\theta_A R_A} = \left(1 - \frac{\theta_B R_B}{\theta_A}\right)$$

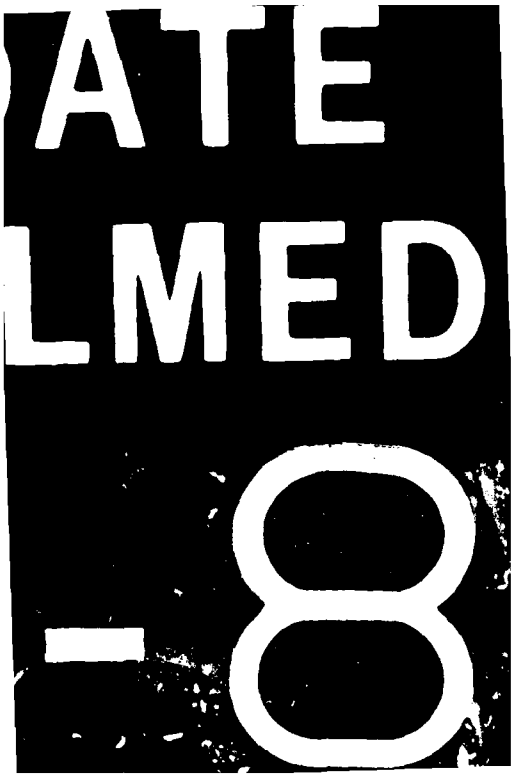
ATE
LMED
-8